

AD-A068 316

VOUGHT CORP ADVANCED TECHNOLOGY CENTER INC DALLAS TEX F/G 1/3
N-RAY INSPECTION OF AIRCRAFT STRUCTURES USING MOBILE SOURCES: A--ETC(U)
APR 79 W D DANCE N68335-77-C-0555

UNCLASSIFIED

ATC-B-92200/8CR-137

NAEC-92-116

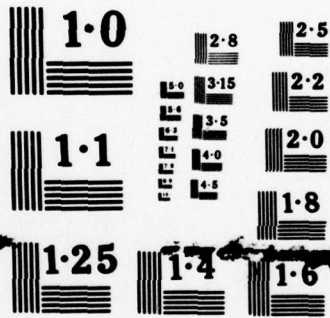
NL

1 OF 1
ADA
088316



END
DATE
FILMED

6 79
DDC



NATIONAL BUREAU OF STANDARDS
MICROCOPY RESOLUTION TEST CHART

THE UNIVERSITY OF ALABAMA
OFFICE OF THE CHIEF OF POLICE
UNIVERSITY OF ALABAMA
TUSCALOOSA, ALABAMA

Approved by: *[Signature]*
F. L. [unclear]
[unclear]
[unclear]

Approved by: *[Signature]*
Richard C. [unclear]
Advanced Technology Section
Training and Servicing/Arms
Division (207)

Approved by: *[Signature]*
F. L. [unclear]
[unclear]
[unclear]

62244N

UNCLASSIFIED

SECURITY CLASSIFICATION OF THIS PAGE (When Data Entered)

REPORT DOCUMENTATION PAGE		READ INSTRUCTIONS BEFORE COMPLETING FORM	
1. REPORT NUMBER NAEC 92-116	2. GOVT ACCESSION NO.	3. RECIPIENT'S CATALOG NUMBER (9)	
4. TITLE (and Subtitle) 6 N-Ray Inspection of Aircraft Structures Using Mobile Sources: A Compendium of Radiographic Results		5. TYPE OF REPORT & PERIOD COVERED Final Rept. 18 May 77 - 22 Dec 78	
7. AUTHOR(s) 10 Dr. W. E. Dance		8. CONTRACT OR GRANT NUMBER(s) 15 N68335-77-C-0555 New	
9. PERFORMING ORGANIZATION NAME AND ADDRESS Vought Corporation Advanced Technology Center, Inc. P. O. Box 226144, Dallas, TX 75266		10. PROGRAM ELEMENT, PROJECT, TASK AREA & WORK UNIT NUMBERS W A3400000/051B/8F41461406	
11. CONTROLLING OFFICE NAME AND ADDRESS Naval Air Systems Command AIR-340E Washington, D. C. 20361		12. REPORT DATE 11 16 Apr 1979	
14. MONITORING AGENCY NAME & ADDRESS (if different from Controlling Office) Naval Air Engineering Center Ground Support Equipment Dept. (Code 92724) Lakehurst, New Jersey 08733		13. NUMBER OF PAGES 49	
		15. SECURITY CLASS. (of this report) UNCLASSIFIED	
16. DISTRIBUTION STATEMENT (of this Report) Approved for Public Release; Distribution Unlimited.		15a. DECLASSIFICATION/DOWNGRADING SCHEDULE	
17. DISTRIBUTION STATEMENT (of the abstract entered in Block 20, if different from Report) 16 F41461 17 WF41461406			
18. SUPPLEMENTARY NOTES			
19. KEY WORDS (Continue on reverse side if necessary and identify by block number) Nondestructive Inspection Mobile N-Ray Neutron Radiography Aircraft Inspection Corrosion Detection Bonded Structures Inspection			
20. ABSTRACT (Continue on reverse side if necessary and identify by block number) This report presents a compendium of typical results of neutron radiographic inspections performed on aircraft structures and laboratory structural specimens. The radiographs are representative of the capability of isotope or small accelerator (nonreactor) neutron sources for imaging defects in aircraft and missile structures. The results show that: (1) the resolution and sensitivity of transportable sources are adequate for effective inspection of structures for many commonly occurring defects (the validity of the			

DD FORM 1 JAN 73 1473

EDITION OF 1 NOV 65 IS OBSOLETE
S/N 0102-LF-014-6601

UNCLASSIFIED

SECURITY CLASSIFICATION OF THIS PAGE (When Data Entered)

389 797

Handwritten signature/initials

SUMMARY

A compendium of typical results of neutron radiographic inspections performed on aircraft structures and laboratory specimens is presented in this report. These results were compiled, documented and presented so as to indicate the capability and limitations of nonreactor, mobile (or potentially portable) sources for effective inspection of specific types of aircraft structures. Neutron sources utilized for the radiographs in the compendium include Californium-252 isotope sources, a Van de Graaff accelerator, and a reactor used in a mode which simulated the beam geometry of a mobile system.

Types of structures represented in the compendium are metal honeycomb, solid metal laminates, mixed metal/composites, and various aircraft members comprising multiple element types. These specimens are representative of structures found in current and proposed Navy aircraft design. The detection of bonding defects in both thin and thick metal laminates, as well as composite-to-metal structures, is demonstrated, as is the imaging of corrosion products in such structures. The specimens inspected include laboratory prepared controls, aircraft experimental structures, and in-service aircraft.

Radiographic features pertinent to the specific specimens were cited, where applicable, to aid in the interpretation of future radiographic results for similar specimens or structures.

Radiographic parameters indicating the conditions of neutron beam exposure were tabulated for ready reference and intercomparison of the radiographs in the compendium, or for comparison to results reported elsewhere.

From observation and analysis of the radiographs, it is concluded that: (1) The resolution and sensitivity of state-of-the-art mobile N-Ray systems are adequate for effective nondestructive inspection of aircraft for many commonly occurring defects; (2) radiographic results from such systems included in the compendium clearly demonstrate the validity and power of the technique; (3) the systems utilized in the exploratory work which provided these results have proved the feasibility of making N-Ray systems sufficiently portable to inspect aircraft structures.

PREFACE

The compilation of N-Ray inspection results by Vought Corporation Advanced Technology Center is intended to illustrate results of neutron radiography techniques for mobile inspection of aircraft structures. The study was performed under the initiation and sponsorship of the Ground Support Equipment Department, Code 92724, of the Naval Air Engineering Center, Lakehurst, NJ, via contract N68335-77-C-0555. Such a compendium with its documentation serves as a basis for evaluating both the capabilities and limitations and hence the overall effectiveness of mobile N-Ray sources for inspection of typical structures. The study also provides a means of intercomparison of radiographic results from various sources and illustrates what differences in results, if any, might be expected due to differences in N-Ray system design and techniques used for imaging. It should also be noted that radiographs presented here show much longer exposure times than could be expected with a mobile N-Ray system which could be currently built. The time frame encompassed on these N-Rays is from about August 1972 to August 1978.

TABLE OF CONTENTS

Section	Subject	Page
	SUMMARY.....	1
	PREFACE.....	2
	LIST OF TABLES.....	4
	LIST OF ILLUSTRATIONS.....	4
I	INTRODUCTION.....	7
II	COMPENDIUM DATA.....	9
III	DISCUSSION.....	11
IV	CONCLUSIONS.....	14
V	RECOMMENDATIONS.....	15
VI	REFERENCES.....	16

LIST OF TABLES

<u>Table</u>	<u>Title</u>	<u>Page</u>
I	RADIOGRAPHIC DATA SOURCE.....	9
II	NEUTRON RADIOGRAPHY SPECIMEN CATEGORIES.....	10
III	CONCEPTUALIZATION OF MOBILE N-RAY SOURCES FOR FIELD INSPECTION OF STRUCTURES.....	12

LIST OF ILLUSTRATIONS

<u>Figure</u>	<u>Title</u>	<u>Page</u>
1	Neutron Radiograph of Aluminum Honeycomb Aircraft Panel Panel - Side 1.....	19
2	Neutron Radiograph of Aluminum Honeycomb Aircraft Panel - Side 2.....	20
3	Neutron Radiograph of Aluminum Honeycomb Specimen - Long Duration Exposure	21
4	Neutron Radiograph of Honeycomb NDI Test Panel No. 1....	22
5	Neutron Radiograph of Honeycomb NDI Test Panel No. 2....	23
6	Neutron Radiograph of Thick Aluminum Adhesively Bonded Butt Joint.....	24
7	Neutron Radiograph of Bonded Thick Aluminum Laminated Test Panel (4 layer).....	25
8	Neutron Radiograph of Adhesively Bonded, Thick Aluminum Wing Skin.....	26
9	Neutron Radiograph of Adhesively Bonded Lap Joint Specimen.....	27
10	Neutron Radiograph of Laminated Skin-to-Spar Joint in Aircraft Wing Section.....	28
11	Fast Film/Converter Neutron Radiograph of Thick Laminated Skin-to-Spar Joint in Aircraft Wing Section...	29
12	Comparison of Neutron and X-Ray Inspection of Hybrid Metal/Composite Wing Skin Structure.....	30
13	Comparison of Neutron and X-Ray Inspection of Missile Combustor Port Cover Assembly.....	31

LIST OF ILLUSTRATIONS (Continued)

<u>Figure</u>	<u>Title</u>	<u>Page</u>
14	Neutron Radiograph of Composite Skin/Aluminum Honeycomb Aircraft Wing Spoiler.....	32
15	Neutron Radiograph of Bonded Composite Specimens.....	33
16	Neutron Radiograph of Graphite Epoxy Specimen Containing Cracks in Sub Layer.....	34
17	Comparison of Neutron and X-Ray Inspection of Corrosion Damaged Aileron Section.....	35
18	Neutron Radiograph of Corroded F-8 Fuselage Panel.....	36
19	Neutron Radiograph of A-7 Nose Gear Housing.....	37
20	Neutron Radiograph of Trunnion Bushing Area in A-7 Nose Gear.....	38
21	Neutron Radiograph of A-7 Nose Gear Corrosion Reference Specimen for Main Bushing Outer Housing.....	39
22	Neutron Radiograph of Stress Corrosion Crack in A-7 Nose Gear Housing.....	40
23	Neutron Radiograph of E-2C Wing Tank Structure.....	41
24	Neutron Radiograph of E-2C Wing Fuel Tank Structure.....	42
25	Neutron Radiograph of C-130 Wing Structure.....	43
26	Neutron Radiograph of Lower Skin of C-130 Aircraft Wing.	44
27	Neutron Radiograph of F-4 Torque Box Panel.....	45
28	Neutron Radiograph of A-5 Aircraft Skin.....	46
29	Neutron Radiograph of a C-2 Vertical Fin, and Fin with Corrosion Penetrameter Attached.....	47
30	Neutron Radiograph of Corrosion Penetrameter, and C-2 Fin with Penetrameter Attached.....	48
31	Transfer Exposure Neutron Radiograph of a Corroded Aluminum Aircraft Skin.....	49

LIST OF ILLUSTRATIONS (Continued)

Page	Title	Figure
32	Neutron Radiograph of Composite Skin/Aluminum Honeycomb Aircraft Wing Speller	14
33	Neutron Radiograph of Bonded Composite Specimens	15
34	Neutron Radiograph of Graphite Epoxy Specimen Containing Cracks in Sub Layer	16
35	Comparison of Neutron and X-Ray Inspection of Corrosion Damaged Aircraft Section	17
36	Neutron Radiograph of Corroded F-8 Fuselage Panel	18
37	Neutron Radiograph of A-7 Nose Gear Housing	19
38	Neutron Radiograph of Trunnion Bushing Area in A-7 Nose Gear	20
39	Neutron Radiograph of Trunnion Bushing Area in A-7 Nose Gear	21
40	Neutron Radiograph of Stress Corrosion Crack in A-7 Nose Gear Housing	22
41	Neutron Radiograph of E-5C Wing Tank Structure	23
42	Neutron Radiograph of E-5C Wing Fuel Tank Structure	24
43	Neutron Radiograph of B-10 Wing Structure	25
44	Neutron Radiograph of Lower Skin of C-130 Aircraft Wing	26
45	Neutron Radiograph of F-4 Torque Box Panel	27
46	Neutron Radiograph of A-5 Aircraft Skin	28
47	Neutron Radiograph of A-2 Vertical Fan and Fin with Corrosion Penetrator Attached	29
48	Neutron Radiograph of Corrosion Penetrator, and C-2 Fin with Penetrator Attached	30
49	Transfer Exposure Neutron Radiograph of a Corroded Aluminum Aircraft Skin	31

THIS PAGE LEFT BLANK INTENTIONALLY.

I. INTRODUCTION

Advanced aircraft structural designs have evolved in recent years which challenge the application of conventional techniques for nondestructive inspection of structures based on these designs. Detection of corrosion in conventional aircraft structures continues to be of prime concern in current aircraft reliability programs and in assessing the serviceability of advanced structural designs.

Neutron radiography (N-Ray) is unique in its ability to accurately image hydrogenous and certain other materials hidden within metallic structures. This selectivity of materials in radiographic imaging provides an inspection tool for potential use in routine inspection of aircraft. Applications include inspection for corrosion, sealant leaks, adhesive bonding defects, accumulation of moisture, and many other defects. For some applications, such as inspection of adhesive bond lines in structures involving complex metal joints, neutron radiography may be the only current effective inspection technique. In other applications for which X-ray is ineffective due to high attenuation in thick metal laminates, conventional ultrasonic techniques may yield useful nondestructive testing (NDT) information. In many such instances, neutron radiography is superior, as it not only detects the presence of flaws but also precisely defines its extent and shape through the shadow imaging process. For inspections where this type of imaging can be applied, neutron radiography offers the promise of significant savings in maintenance costs, since a large portion of the work load in today's maintenance programs is in disassembling the aircraft to permit routine inspections or to find the cause of malfunctions. It is in this area that "shortcuts" are sorely needed, provided of course, that they are valid and dependable.

In the time frame of the evolution of advanced aircraft structural designs, the capabilities and scope of application of neutron radiography have expanded through the increased availability of nonreactor neutron sources, which lend themselves to transportable neutron radiography. Considerable effort has been expended in recent years to evaluate the applicability of neutron radiography to on-site inspection of aircraft and for solving some of the more difficult inspection problems (references (a) through (r).) Numerous experiments have demonstrated the ability of the neutron radiographic technique to image flaws which defy detection by more conventional means.

It is the objective of this study to present a compendium of results from neutron radiography inspections performed on aircraft structures and laboratory specimens by isotope or accelerator neutron sources. The purpose of the compendium is to present and document the results from various experimental efforts in such a manner as to indicate the capability and limitations of mobile neutron radiography for inspection of specific types of structures. The results as documented will aid in the interpretation of results from similar future inspections. Examples will be presented for structures for which the suitability of the technique for inspection has been proven. In addition, examples will be cited for which the suitability appears promising but where additional work is deemed necessary to establish its ultimate effectiveness for routine inspections.

While it is recognized that neutron radiography is not a panacea for detecting all types of structural defects, it is anticipated that the technique will play a significant role in assessing the serviceability of Navy aircraft, whether they be in-service aircraft such as the E-2, F-4, F-14 and A-7 or the advanced F-18 and AV-8, or future aircraft such as the VSTOL Type A or B projected for the 1990's. This study is designed to aid in determining the nature of this role, as well as the role that the technique will assume in intermediate-level maintenance of aircraft in the fleet.

II. COMPENDIUM DATA

The organizations that provided radiography results for this study, along with the types of neutron sources used to attain the results, are listed in Table I.

In compiling the radiographic data, a concerted effort has been made to include data from different types of portable or nonreactor neutron sources in current usage, as well as from different facilities of the same type.

The selection of types of radiographs is not intended to be all inclusive in scope. The collection of radiographs was limited to a manageable number which illustrate the type of results available for selected structures. The radiographs are grouped as shown in Table II.

The radiographs are shown in Figures 1 through 31. Without exception, the radiographs are presented as positive prints of the original negatives. Hence, the darker areas in the print represent greater neutron attenuation in the specimen, and the lighter areas correspond to greater neutron transmission. Pertinent exposure data and interpretation information for the radiographs are provided for easy reference either on the page with the figure or on the page facing the figure.

TABLE I. RADIOGRAPHIC DATA SOURCE

<u>Organization</u>	<u>Types of Neutron Sources</u>	<u>References</u>
Vought Corporation Advanced Technology Center, Inc. (ATC)	a. Californium-252, < 3 milligrams b. Van de Graaff Ac- celerator, 3 MeV	(a) - (i)
IRT Corporation (IRT)	Californium-252, ≤ 10 milligrams	(j) - (p)
National Bureau of Standards (NBS)	Reactor, 10MW, L/D reduced to ~40 to simulate nonreactor radiography	(q)
Royal Military College of Canada (RMC)	Californium-252, 2 milligrams	(r)

TABLE II. NEUTRON RADIOGRAPHY SPECIMEN CATEGORIES

	<u>Radiograph No.</u>
Adhesively Bonded Metal Structures:	1-11
Aluminum Honeycomb	1-5
Solid Laminates	6-9
Closed Wing Structures	10-11
Composite Structures:	12-16
Composite/Metal Structures	12-15
Graphite Epoxy Structural Materials	15-16
Corrosion:	17-31
In-Service Structures	17-20, 22-28, 31
Laboratory Specimens	21, 29, 30

III. DISCUSSION

A. CAPABILITY ASSESSMENT. Observations from the analysis of radiographs in this compendium and from the referenced reports demonstrate that mobile neutron radiography is highly effective for assessing adhesive bond-line quality in metallic and composite/metallic structures, even through thick metal structures and complex joints. Additionally, internal sealant distribution within metallic structures is accurately imaged, providing capability for detecting fuel tank leakage paths, position and condition of O-ring seals, etc. Corrosion products and other effects of corrosion in metallic members are discernible with good sensitivity. Hydroxides and chlorides resulting from the corrosion process are readily imaged in the absence of other hydrogenous materials, and less easily in the presence of such materials. However, discrimination between corrosion products and other hydrogenous materials such as water, oils and sealants is possible in most cases through pattern recognition and analytical techniques. Also, significant potential exists for process flaw detection in composite materials and structures through mobile neutron radiography.

Through use of appropriate imaging film/converter combinations, flaw resolution capability of 1/8 inch in difficult structures is readily attainable with exposure times of five to ten minutes using state-of-the-art mobile neutron sources. This capability is adequate for many types of aircraft inspection problems. For resolution higher than that stated above, greater source-to-specimen distances must be used for proper imaging. This requirement necessitates higher neutron intensity than is generally feasible with current mobile sources. Thus, if rapid imaging with high resolution is a requirement, a fixed-base reactor, accelerator or ^{252}Cf multiplier system is needed.

This compendium of radiographs demonstrates the validity and power of the neutron radiography inspection technique, and the systems which provided the compendium radiographs demonstrate the feasibility of making N-Ray operations "mobile" for practical inspection situations. The reduction in aircraft maintenance manhours and thus maintenance cost which is potentially available through mobile N-Ray may be realized only through implementing the transition from exploratory N-Ray work to a real-world, routine aircraft inspection capability. This will be accomplished through development of specialized equipment for adapting the N-Ray technique to a routine field process analogous to that used in X-ray inspection.

B. APPROACH. The type of neutron source recommended for achieving the objective of a safe, mobile N-Ray system for routine inspections is an "on-off" ion accelerator neutron generator. The use of large ^{252}Cf sources for rapid inspection becomes less practical for mobile applications as the required shielding weight for the stored source increases. In high resolution or short exposure applications requiring higher flux than that available from a few milligrams of ^{252}Cf (2.3×10^9 n/sec per milligram), the concept of a mobile accelerator system becomes attractive as an alternative technique. Mobile accelerator sources capable of supplying in excess of 5×10^{10} neutrons/second are commercially available. In comparison with a 3-milligram ^{252}Cf system, for example, it is estimated that exposures would

be approximately five times as fast. An inspection requiring one hour for a given resolution using the 3-mg ^{252}Cf system would require only 12 minutes with the accelerator system.

For field inspection applications, potential advantages of such a source over isotope sources lie in the areas of: (1) speed, (2) mobility, (3) costs, and (4) on-off operation. More specifically, the most significant cost saving compared with isotope sources lies in the initial cost of the neutron source. Rough estimates for the two types of sources are compared, for example, in Table III. The cost estimates are for the basic mobile source with basic positioning device and include, in the case of the isotope, the biological shielding required for the residual source (not required with accelerator source). Savings in recurring costs would be highly dependent on the extent or pattern of neutron beam utilization from the system, i.e., the long-term duty cycle of the system. A comparison of recurring costs, for example, must be based chiefly on the costs of isotope replacement per inspection performed (which, in the case of an isotope system, is strongly dependent on time utilization of the decaying isotopic beam) versus the cost of tube replacement per inspection (which, in the case of an accelerator system, is independent of the time utilization, as the tube lifetime is dependent only on tube "on-time").

Not to be underestimated as a distinct advantage of an accelerator system over an isotope system is the convenience of being able to turn off all external radiation when the system is not in use. This aspect overcomes the psychological barrier that exists in many instances due to the radiation emitted external to the shielding of a continuously emitting isotope source and simplifies the radiation safety procedures, particularly for field inspection applications.

TABLE III. CONCEPTUALIZATION OF MOBILE N-RAY SOURCES FOR FIELD INSPECTION OF STRUCTURES

Accelerator Neutron Output (n/sec)	Californium-252 Equivalent (mg) (After Thermalization)	Typical Film Exposure Times (AA)	Estimated Source Parameters (Basic Mobile Source With Shield)			
			Portable Accelerator System		Californium-252 System	
			Cost (\$K)	Weight (Lb)	Cost (\$K)	Weight (Lb)
10^9	~ 0.3	30 hrs	75	1,000	50	1,500
10^{10}	~ 2.8	3 hrs	125	3,000	125	5,000
10^{11}	~ 27.2	18 min	300	8,000	500	30,000

C. CURRENT STATE-OF-THE-ART. The Vought Corporation Advanced Technology Center has developed the concept of a transportable "on-off" N-Ray System based on a sealed tube ion accelerator neutron generator.

Under contract (DAAG46-78-C-0007) with the Army Materials and Mechanics Research Center, Watertown, MA, Vought is currently providing the Army with an engineering model of this system. This device will be the first of its kind and much information relating to operating parameters, physical/functional features, and capabilities will be learned during its development and evaluation. Manufacture of this device should be completed by July 1979 with engineering testing to follow.

D. COST AND RISK. In general, the cost and risk associated with the on-going technology of an "on-off" mobile system are relatively high since this development involves a new methodology in neutron radiography. There is, however, sufficient background information and experience to assume a good probability for producing a viable system which will add an important method to the aircraft inspection scene. Because of the cost and risk involved, coordination of on-going development of this technique within DOD is warranted. The coordinated effort should reduce duplication of effort, and give each service a voice in the developmental effort while distributing the total expenditure.

IV. CONCLUSIONS

A. Mobile neutron radiography has been shown to be highly effective as a nondestructive testing technique for: (1) locating corrosion and internal sealant distributions in metallic structures; (2) assessing adhesive bond line quality in metallic/composite structures; (3) locating hydrogenous materials such as water, oils and O-rings/seals, etc. (paragraph III.A.).

B. Significant potential exists for detection of certain flaws in composite materials (paragraph III.A.).

C. An "on-off" mobile neutron radiography system with relatively good resolution capability is feasible and may well be cost effective when compared with the necessity of disassembling complex aircraft structures for inspection (paragraph III.B.).

D. An "on-off" N-Ray system is preferable to a system using the Californium isotope in regard to both economics and safety (paragraph III.B. and Table III.).

V. RECOMMENDATIONS

A. Because of the ability of mobile N-Ray to perform specific inspection tasks which could significantly reduce manhour requirements for disassembly-for-inspection methods currently in use and tedious scanning requirements of other NDT methods, especially for corrosion detection (a significant problem in the Naval aviation environment), a mobile N-Ray system should be pursued. It should be pursued, however, with a thorough understanding of its advantages, disadvantages, and cost. These general recommendations for pursuing such a system are:

1. Pursue the "on-off" type ion accelerator neutron generator system because of economics and safety considerations.
2. Promote state-of-the-art research and development to refine the "on-off" system design and capabilities.
3. Monitor development and testing of mobile "on-off" N-Ray systems.
4. Assess the Naval aviation maintenance environment (both intermediate and depot levels) for impact of the use of such a system, and assess the economic feasibility of operation when compared with manhours saved after sufficient information is gained from actual operation of developmental systems.
5. Coordinate development efforts to the largest extent possible with the Army and Air Force to insure accurate capability assessment and most effective use of manpower and funds.

VI. REFERENCES

- (a) Dance, W. E., "Neutron Radiographic Nondestructive Evaluation of Aerospace Structures", ASTM Special Technical Publication STP 586, 1976, pp 137-151.
- (b) Dance, W. E., Soffel, A. R. and Petersen, D. H., "Adhesive Modification for Image Enhancement in the Neutron Radiographic Detection of Bondline Flaws", Vought Corporation ATC Report No. B-94200/4TR-28, Sep 1974.
- (c) Dance, W. E., "Nondestructive Inspection of an Advanced Adhesive Bonded Metallic Primary Wing Structure by Portable Neutron Radiography", Vought Corporation ATC Report No. B-94400/7TR-4, Jan 1977.
- (d) Dance, W. E. and Petersen, D. H., "Verification of the Structural Integrity of Laminated Skin-to-Spar Adhesive Bondlines by Neutron Radiography", Vought Corporation ATC Report, Proceedings of the Symposium on Durability of Adhesive Bonded Structures, U. S. Army Armament Research and Development Command, 27-29 Oct 1976; Journal of Applied Polymer Science: Applied Polymer Symposium 32, 399-410 (1977).
- (e) Dance, W. E., "A Portable Accelerator Neutron Radiography System - Preliminary Feasibility Study", Vought Corporation ATC Report No. B-94400/6TR-8, Jun 1976.
- (f) Dance, W. E., "Evaluation of Mobile ^{252}Cf Neutron Radiography for Field Inspection of Aerospace Structures, U. S. ERDA Fifth ^{252}Cf Utilization Meeting, 4-6 Nov 1975, Californium-252 Progress, No. 20, Jan 1976.
- (g) Dance, W. E., "Evaluation of ^{252}Cf Neutron Radiography for Inspection of Aerospace Structures", Californium-252 Progress, Nos. 12-22, 1972-1978.
- (h) Petersen, D. H. and Dance, W. E., "Neutron Radiographic Techniques for Inspection of Polymeric Materials", Proceedings of the Conference on Critical Review of Techniques for the Characterization of Polymeric Materials", TTCP-3 Program, Army Materials and Mechanics Research Center, 6-8 Jul 1976.
- (i) Dance, W. E. and Middlebrook, J. B., "Neutron Radiographic NDI for Bonded Composite Structures," Proceedings of ASTM Committee D-30 Symposium on Nondestructive Evaluation and Flaw Criticality for Composite Materials, Philadelphia, 10-11 Oct 1978, to be published.
- (j) John, Joseph, Rundquist, D. E., and Sharp, R., "Application of Neutron Radiography Techniques for Nondestructive Detection of Corrosion in Naval Aircraft and Aircraft Components," IRT Corporation Technical Report INTEL-RT 6044-002, Mar 15, 1974.
- (k) Larsen, J. E., Rundquist, D. E., Baltgalvis, J., and John, Joseph, "Investigation of Neutron Radiography Techniques for Corrosion Inspection of A-7 Nose Landing Gear," IRT Corporation Technical Report INTEL-RT 6071-001, Aug 16, 1974.

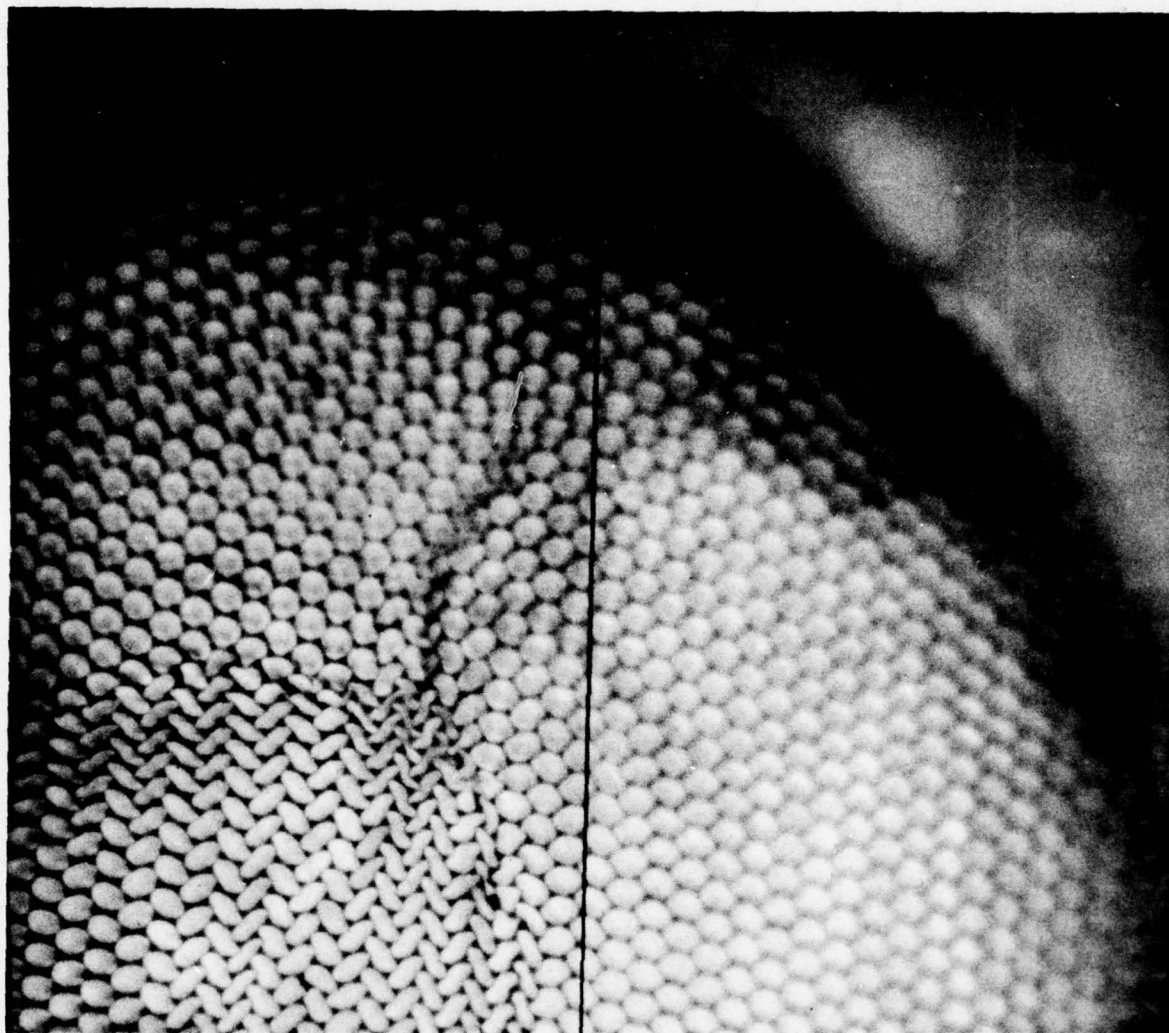
- (l) Larsen, J. E., Baltgalvis, J., Patricelli, F., Gallardo, M., and John, Joseph, "Evaluation of a Portable Neutron Radiographic System for the Detection of Hidden Corrosion in the Wing Fuel Tank of the E-2C Aircraft," IRT Corporation Technical Report INTEL-RT 6082-001, Feb 25, 1975.
- (m) Larsen, J. E., Parks, R., Baltgalvis, J., and John, Joseph, "Investigation of Neutron Radiographic Techniques for Maintenance Inspection of Air Force Aircraft," IRT Corporation Technical Report INTEL-RT 6081-001, Mar 3, 1975.
- (n) Patricelli, F., Larsen, J. E., Baltgalvis, J., and John, Joseph, "Experimental Evaluation of Neutron Radiography for Quantitative Determination of Corrosion in Aircraft Structure," IRT Corporation Technical Report INTEL-RT 6093-001, Jan 28, 1976.
- (o) Harper, H., Baltgalvis, J., Weber, H., and John, Joseph, "Quantitative Determination of Corrosion Using Neutron Radiography," IRT Corporation Technical Report INTEL-RT 6119-001, Jul 30, 1976.
- (p) Harper, H., Stokes, J., Weber, H., and John, Joseph, "Neutron Radiography Study of an F111 Upper Aft Fuselage Panel," IRT Corporation Technical Report IRT 6182-001.
- (q) Garrett, Donald A., "The Macroscopic Detection of Corrosion in Aluminum Aircraft Structures with Thermal Neutron Beams and Film Imaging Methods", NBSIR 78-1434, Dec 7, 1977.
- (r) Bennett, L. D., Royal Military College of Canada, Private Communication, Jul 1978.



SPECIMEN THICKNESS	TYPE AND STRENGTH OF SOURCE	L/D RATIO	CONVERTER FILM COMBINATION	EXPOSURE TIME OR FLUENCE	RADIOGRAPH ORIGIN
1.1"	^{252}Cf , 1.5 mg	18	Gd/M	16 Hr	ATC

The area of chief interest in this radiograph is that showing the condition of the bond line in the honeycomb closeout region. Many adhesive voids are present in this area (indicated by the arrows). The aluminum core was resin-coated in this case.

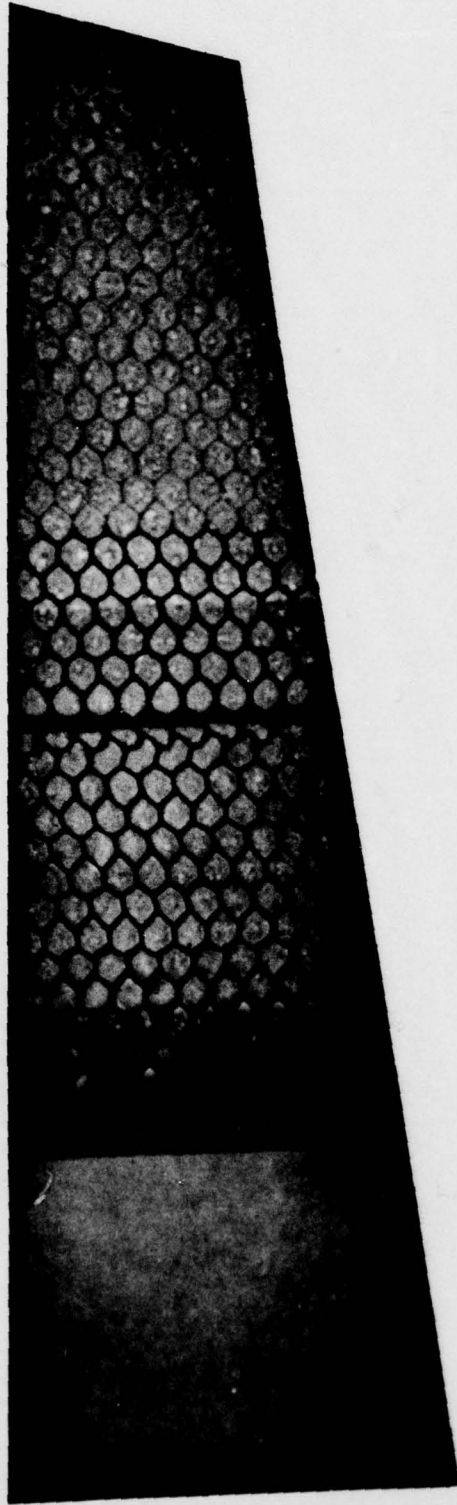
Figure 1 - Neutron Radiograph of Aluminum Honeycomb Aircraft Panel - Side 1



SPECIMEN THICKNESS	TYPE AND STRENGTH OF SOURCE	L/D RATIO	CONVERTER FILM COMBINATION	EXPOSURE TIME OR FLUENCE	RADIOGRAPH ORIGIN
1.1"	²⁵² Cf, 1.5 mg	18	Gd/AA	5 Hr	ATC

The skin-to-core interface on the opposite side of the panel of Figure 1 is shown here. This side, which was not "in focus" in Figure 1 now appears as a sharp image, illustrating the selectivity of imaging resulting from this type of radiographic system.

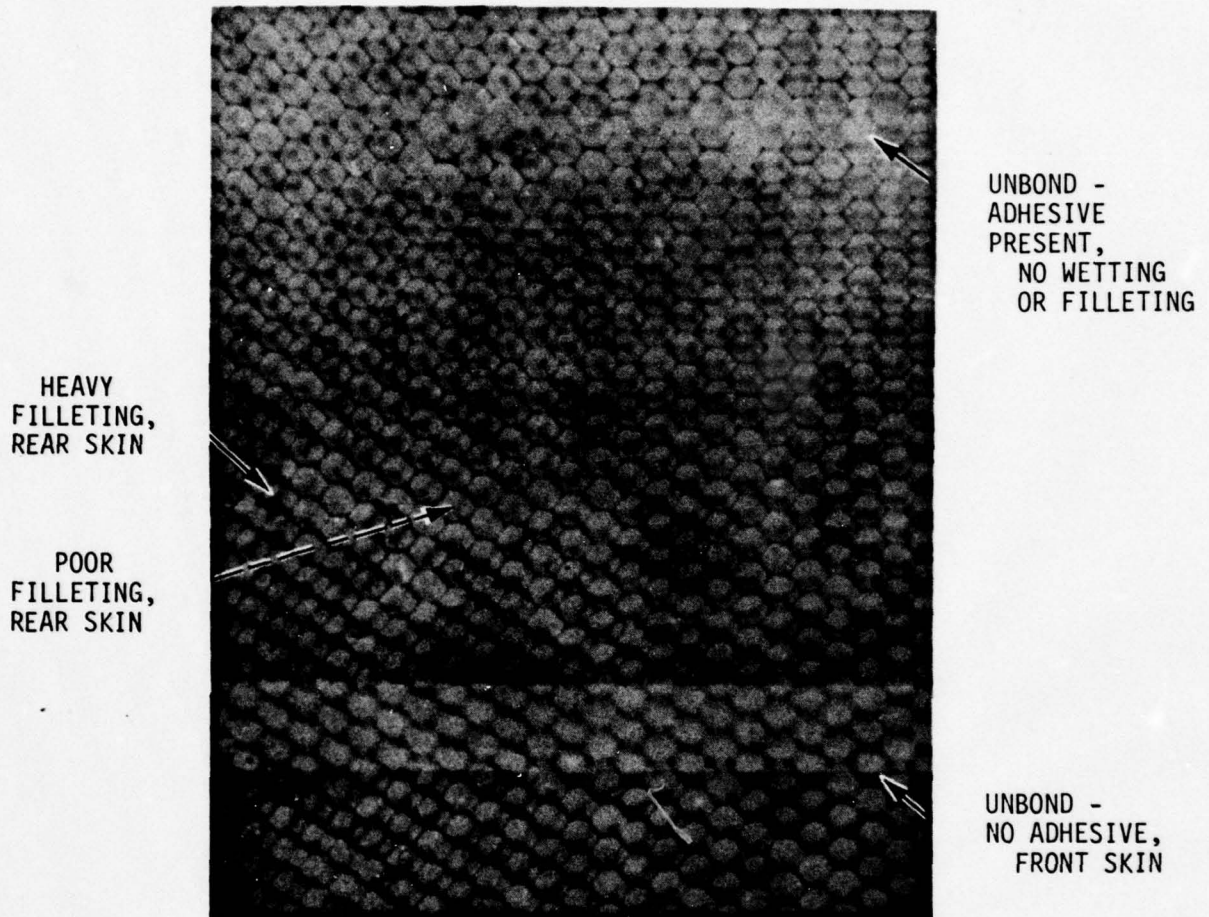
Figure 2 - Neutron Radiograph of Aluminum Honeycomb Aircraft Panel - Side 2



SPECIMEN THICKNESS	TYPE AND STRENGTH OF SOURCE	L/D RATIO	CONVERTER FILM COMBINATION	EXPOSURE TIME OR FLUENCE	RADIOGRAPH ORIGIN
.425"	^{252}Cf , 1.5 mg	32	Gd/SR-54	117 Hr	ATC

This radiograph illustrates the detail attainable in a honeycomb structure with even small quantities of ^{252}Cf , through long-duration exposures.

Figure 3 - Neutron Radiograph of Aluminum Honeycomb Specimen - Long Duration Exposure

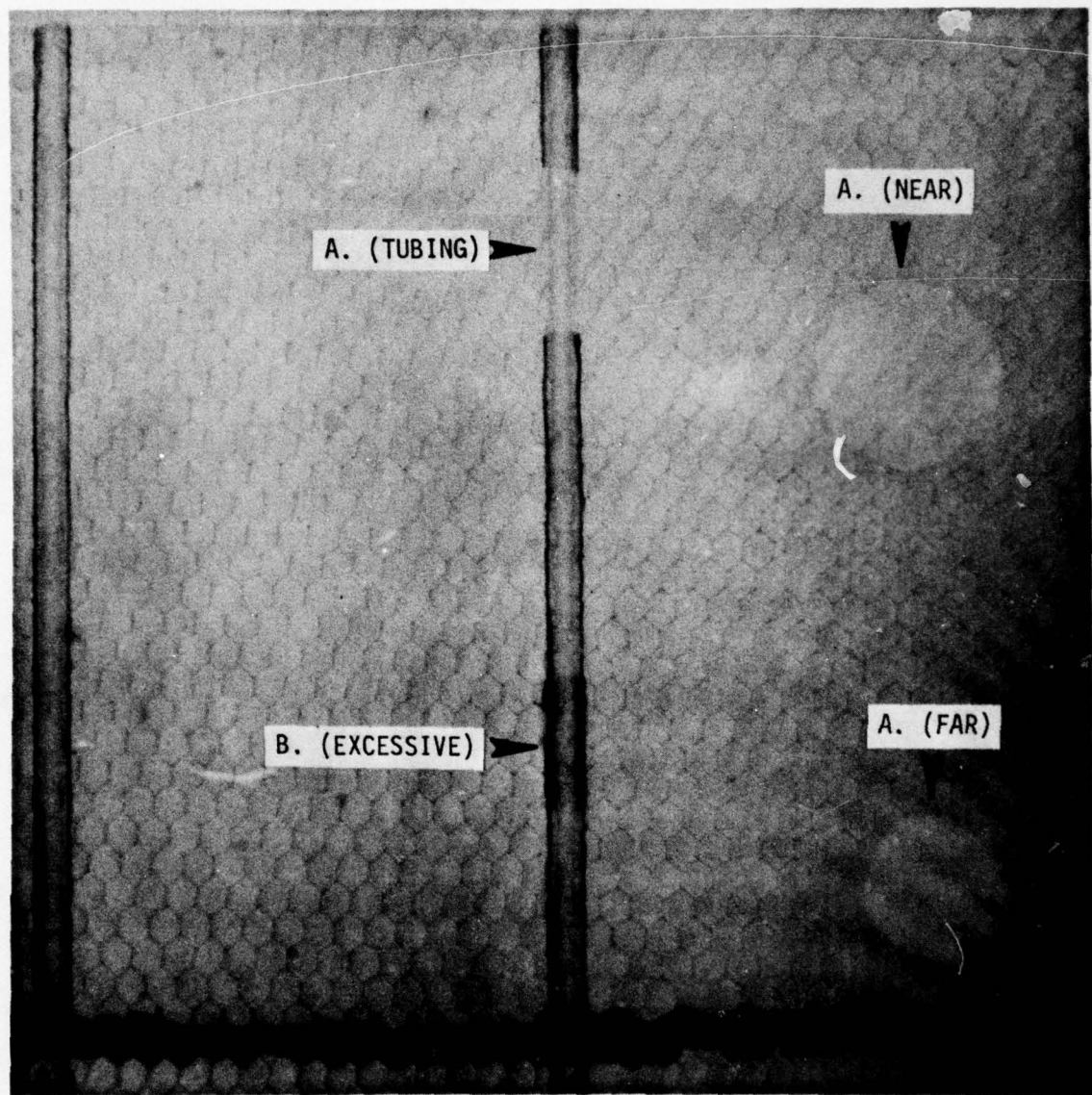


SPECIMEN THICKNESS	TYPE AND STRENGTH OF SOURCE	L/D RATIO	CONVERTER FILM COMBINATION	EXPOSURE TIME OR FLUENCE	RADIOGRAPH ORIGIN
1.125"	²⁵² Cf, 1.0 mg	18	Gd/SR-54	24 Hr	ATC

In this NDI test panel, built-in voids and unbonds are radiographically imaged in the areas indicated:

- a. Unbond prepared by application of thin mylar film between adhesive and face sheet on side of test panel next to imaging cassette.
- b. Unbond prepared by deletion of adhesive between core and face sheet on side of panel next to imaging cassette.

Figure 4 - Neutron Radiograph of Aluminum Honeycomb NDI Test Panel No. 1



SPECIMEN THICKNESS	TYPE AND STRENGTH OF SOURCE	L/D RATIO	CONVERTER FILM COMBINATION	EXPOSURE TIME OR FLUENCE	RADIOGRAPH ORIGIN
--	²⁵² Cf, 2.9 mg	18	Gd/SR-54	24 Hr	ATC

Prepared bond-line flaws in this NDI test panel are imaged in the areas noted:

a. Adhesive deficiency in near skin-to-core bond line, in far skin-to-core bond line, and in tube bonding.

b. Excessive adhesive in tube-to-core bond.

Figure 5 - Neutron Radiograph of Aluminum Honeycomb NDI Test Panel No. 2



SPECIMEN THICKNESS	TYPE AND STRENGTH OF SOURCE	L/D RATIO	CONVERTER FILM COMBINATION	EXPOSURE TIME OR FLUENCE	RADIOGRAPH ORIGIN
0.5"	²⁵² Cf, 2.0 mg	19	Gd/SR-54	22 Hr	ATC

This neutron radiograph illustrates the imaging of flaws in a "difficult-to-inspect" thick aluminum adhesively bonded joint. The specimen was a butt joint comprised of 0.5-inch adherends with a .008-inch thick bond-line.

Figure 6 - Neutron Radiograph of Thick Aluminum Adhesively Bonded Butt Joint

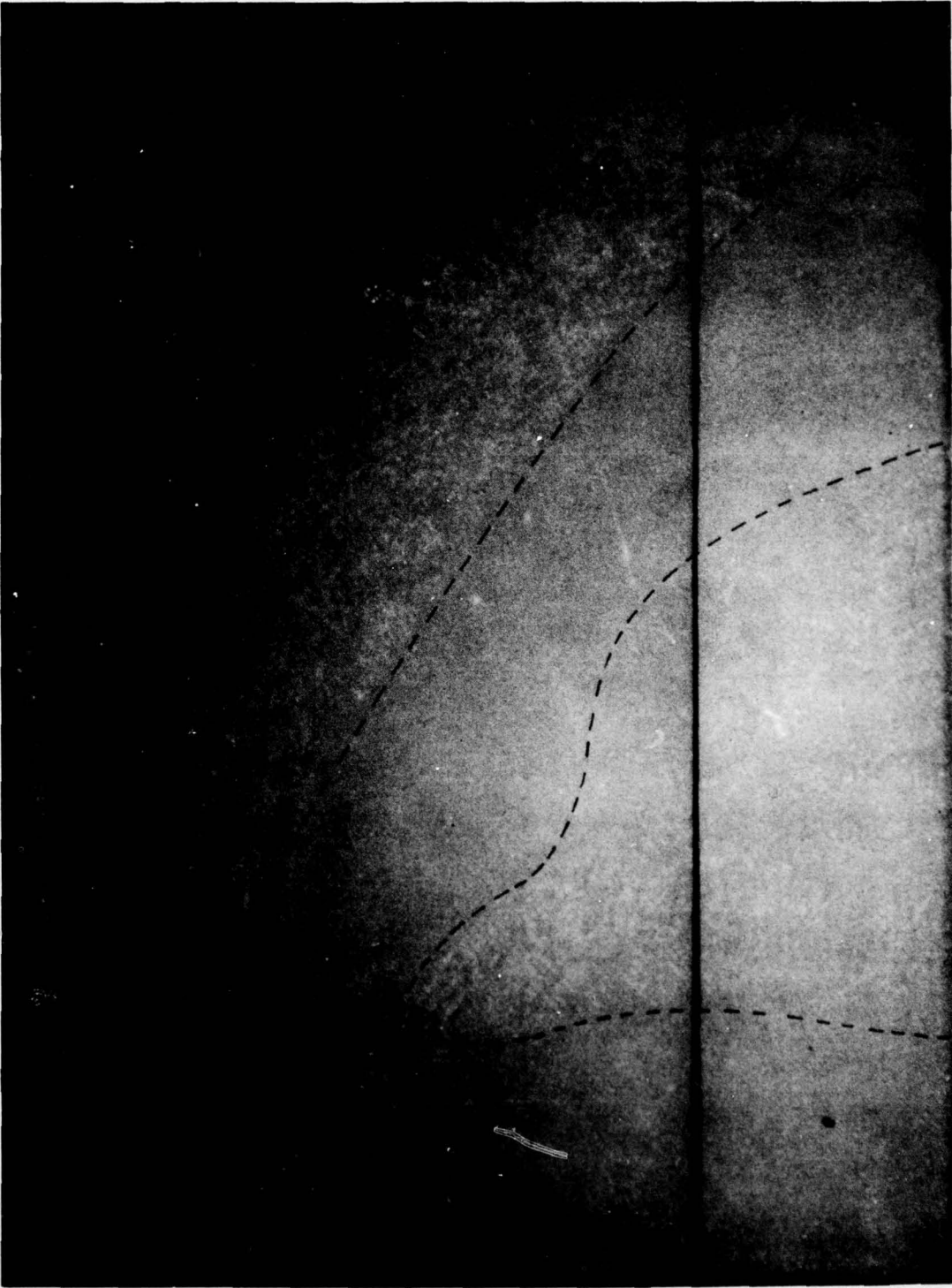


Figure 7 - Neutron Radiograph of Bonded Thick Aluminum Laminated Test Panel (4 Layer)

Figure 7 Comments (opposite page)

SPECIMEN THICKNESS	TYPE AND STRENGTH OF SOURCE	L/D RATIO	CONVERTER FILM COMBINATION	EXPOSURE TIME OR FLUENCE	RADIOGRAPH ORIGIN
0.5"	²⁵² Cf, 3.2 mg	32	Gd/SR-54	60h	ATC

Bond-line porosity in a multilayer laminate is imaged in this aircraft wing skin assembly consisting of four layers of aluminum with 0.5-inch total metal thickness.

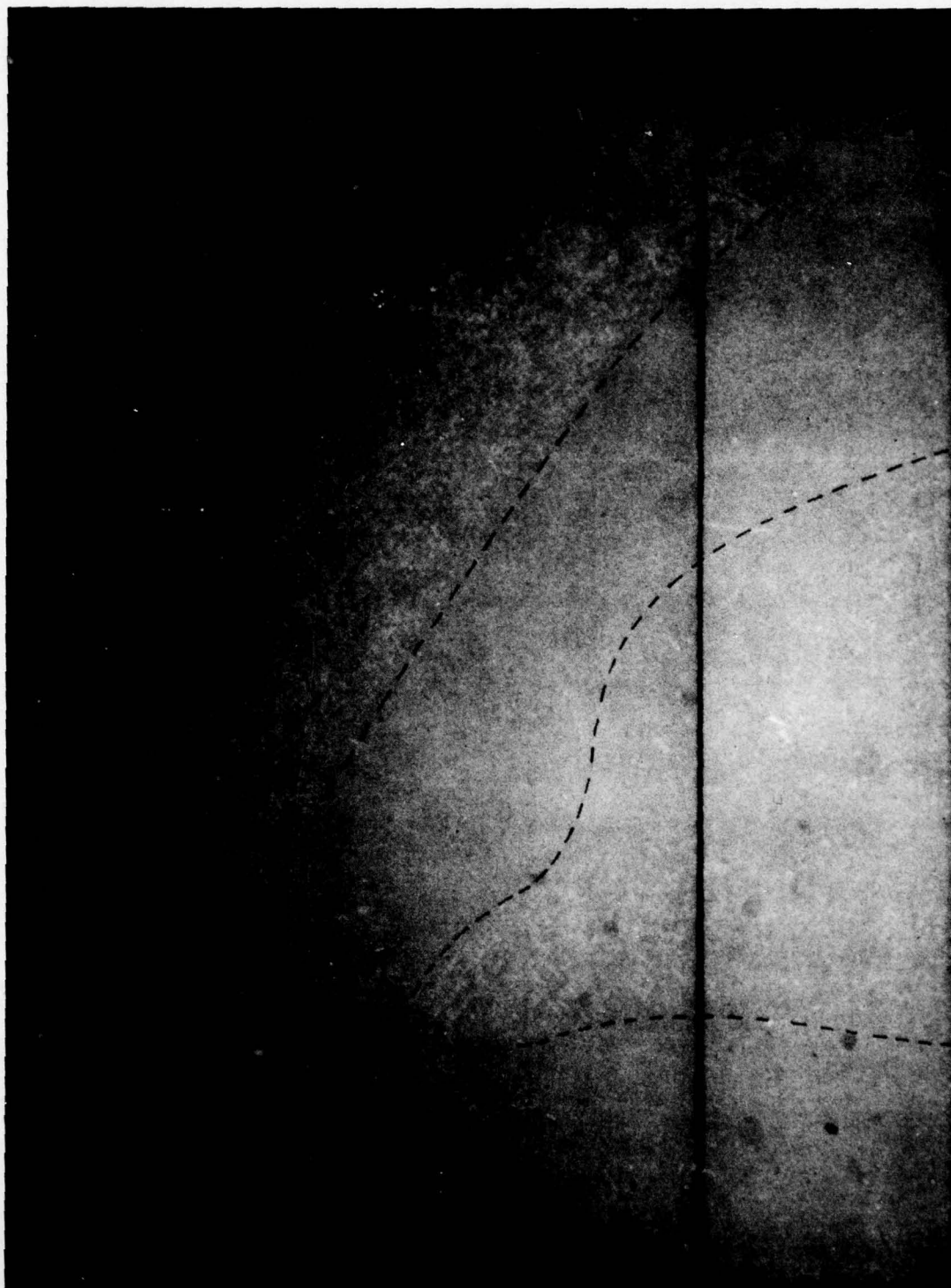
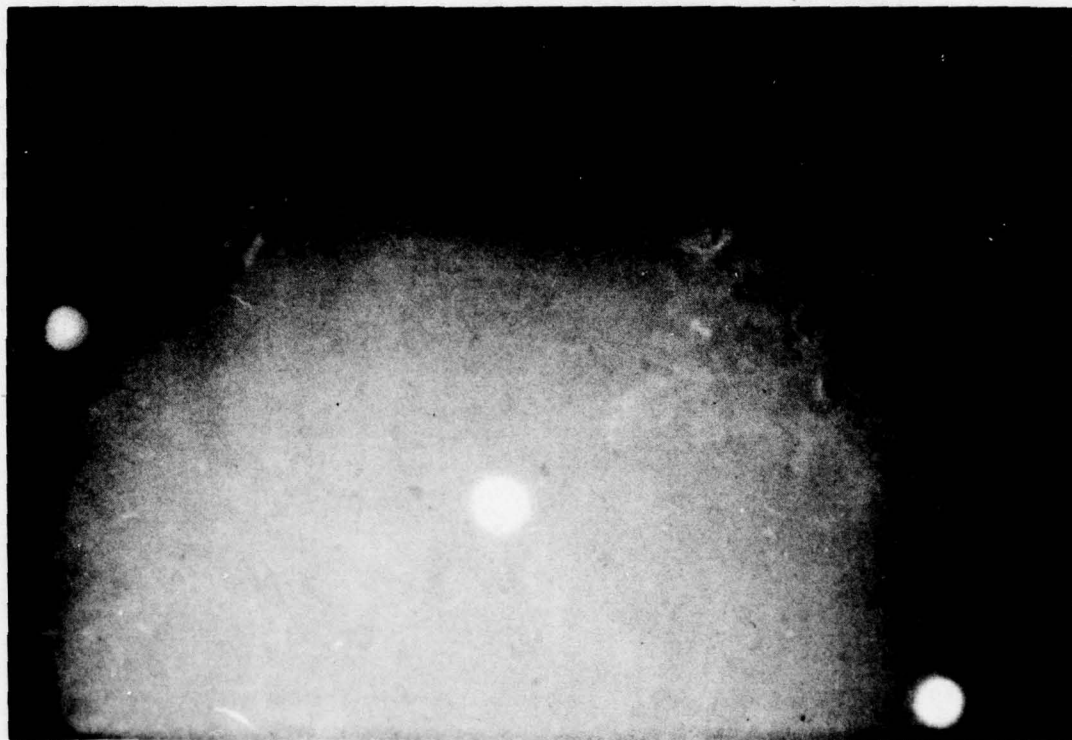


Figure 7 - Neutron Radiograph of Bonded Thick Aluminum Laminated Test Panel (4 Layer)



SPECIMEN THICKNESS	TYPE AND STRENGTH OF SOURCE	L/D RATIO	CONVERTER FILM COMBINATION	EXPOSURE TIME OR FLUENCE	RADIOGRAPH ORIGIN
0.5"	^{252}Cf , 3.1 mg	13	Gd/T	3 Hr	ATC

Gross voids in a multilayer aluminum wing skin bonding are imaged in this neutron radiograph.

Figure 8 - Neutron Radiograph of Adhesively Bonded, Thick Aluminum Wing Skin



SPECIMEN THICKNESS	TYPE AND STRENGTH OF SOURCE	L/D RATIO	CONVERTER FILM COMBINATION	EXPOSURE TIME OR FLUENCE	RADIOGRAPH ORIGIN
.210"	²⁵² Cf, 2.5 mg	22	Gd/SR-54	65 Hr	ATC

This radiograph images numerous small voids in an 0.008-inch adhesive bond line joining two 0.080-inch aluminum adherends.

Figure 9 - Neutron Radiograph of Adhesively Bonded, Thick Aluminum Lap Joint Specimen

TABLE 2 - Description of specimens

Specimen	Material	Thickness	Orientation	Exposure Time	Developer
8" (Wing Thickness)	252Cf, 3.1 mg	8"	Vertical	5.3 Hr	ATC

Figure 10 Comments (opposite page)

SPECIMEN THICKNESS	TYPE AND STRENGTH OF SOURCE	L/D RATIO	CONVERTER FILM COMBINATION	EXPOSURE TIME OR FLUENCE	RADIOGRAPH ORIGIN
8" (Wing Thickness)	²⁵² Cf, 3.1 mg	21	Gd/AA	5.3 Hr	ATC

This radiograph resulted from inspecting a complex joint in a thick laminated aircraft wing section. The area of interest is the laminated skin-to-spar bond line, which is critical to the structural integrity of the wing. A void in this bond line is imaged (arrow).

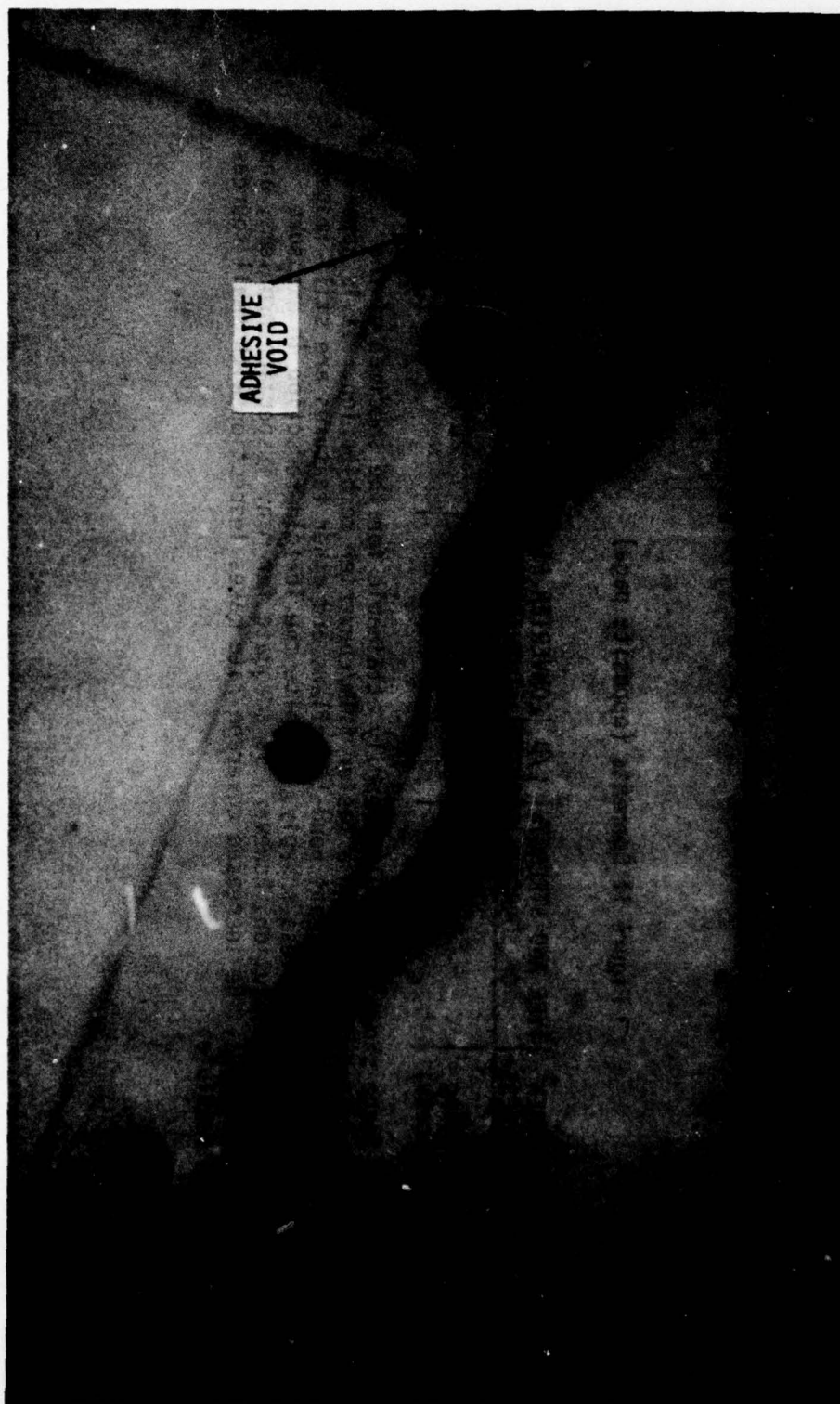


Figure 10 - Neutron Radiograph of Laminated Skin-to-Spar Joint in Aircraft Wing Section

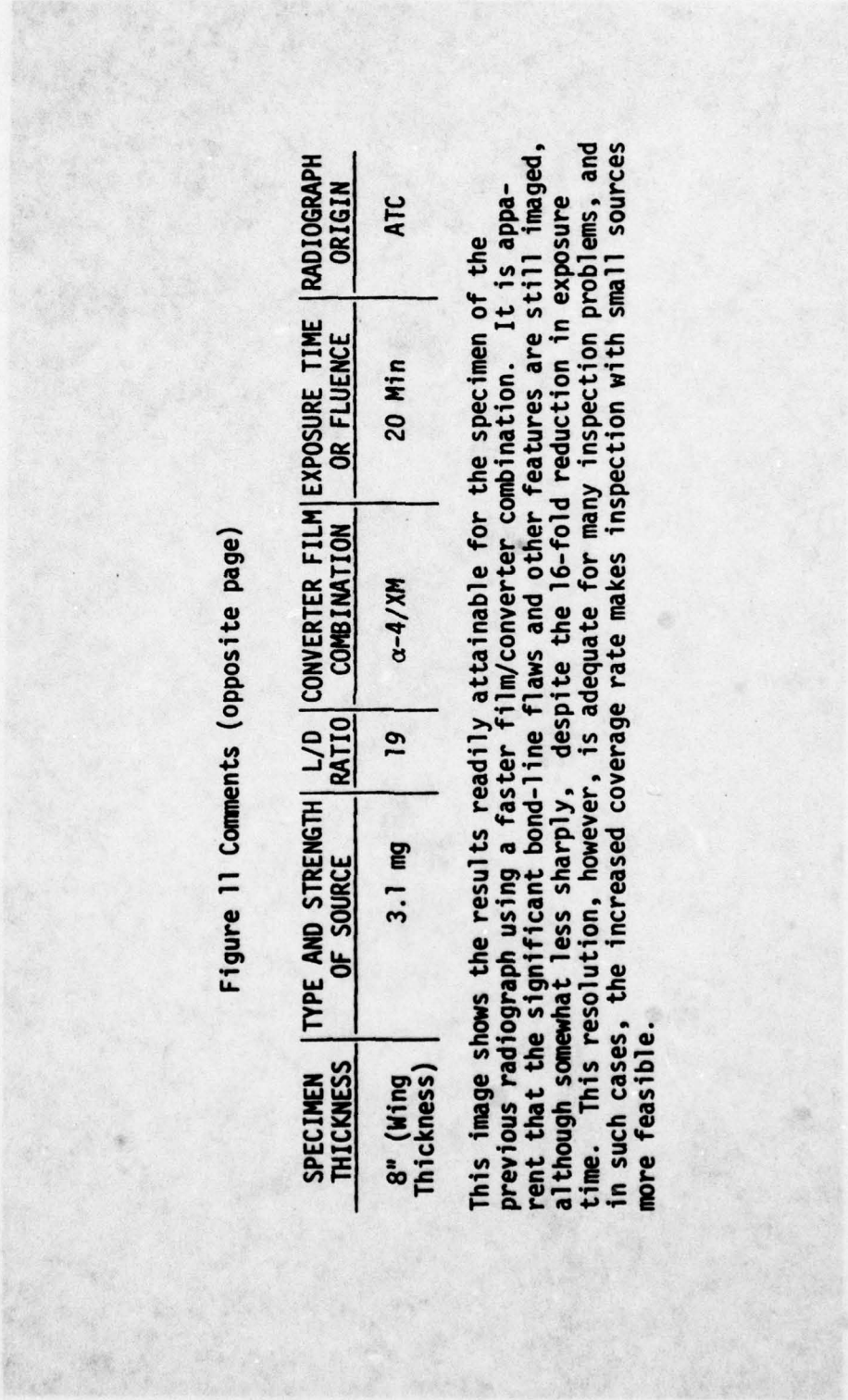


Figure 11 Comments (opposite page)

SPECIMEN THICKNESS	TYPE AND STRENGTH OF SOURCE	L/D RATIO	CONVERTER FILM COMBINATION	EXPOSURE TIME OR FLUENCE	RADIOGRAPH ORIGIN
8" (Wing Thickness)	3.1 mg	19	α-4/XM	20 Min	ATC

This image shows the results readily attainable for the specimen of the previous radiograph using a faster film/converter combination. It is apparent that the significant bond-line flaws and other features are still imaged, although somewhat less sharply, despite the 16-fold reduction in exposure time. This resolution, however, is adequate for many inspection problems, and in such cases, the increased coverage rate makes inspection with small sources more feasible.

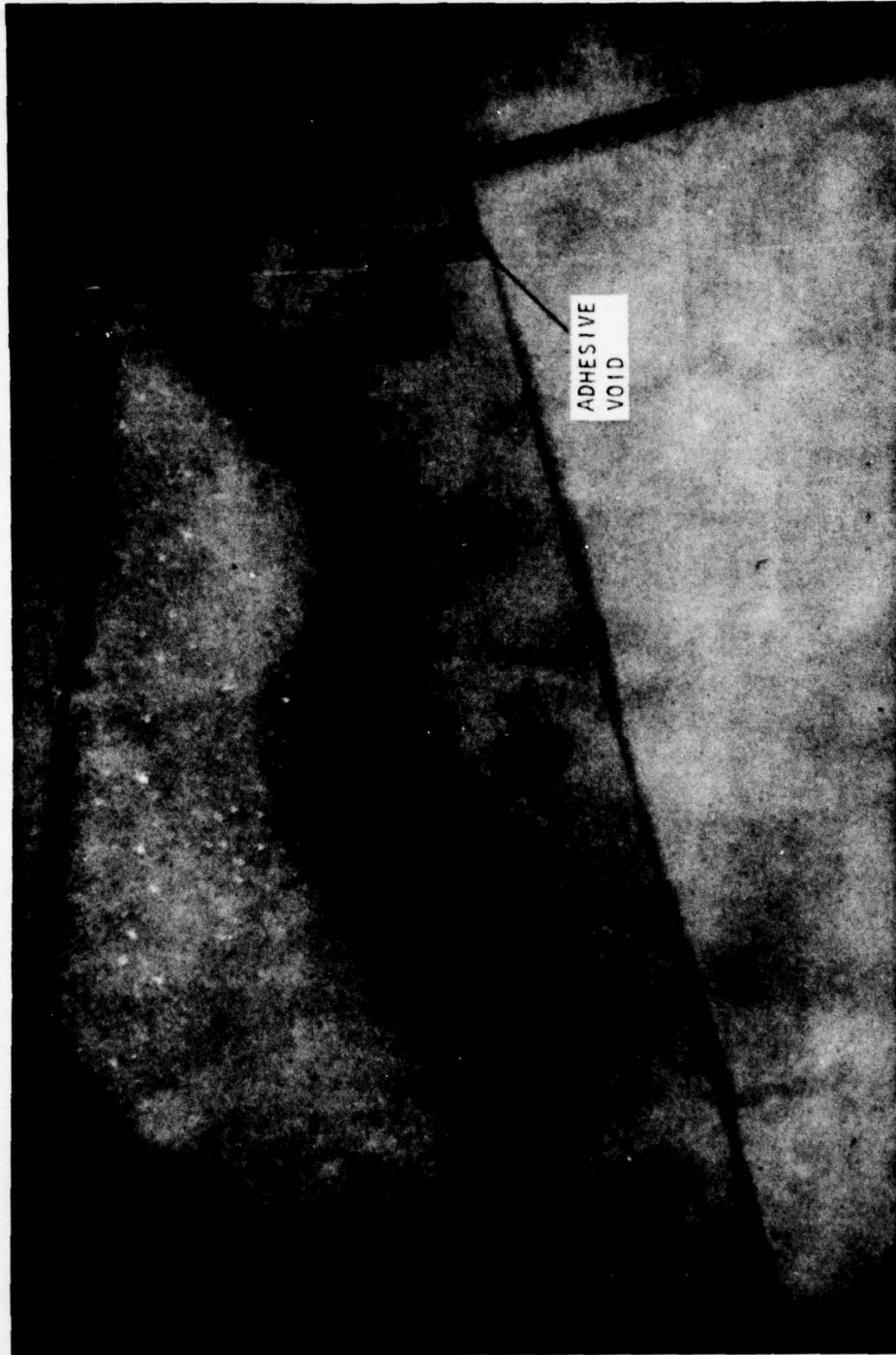
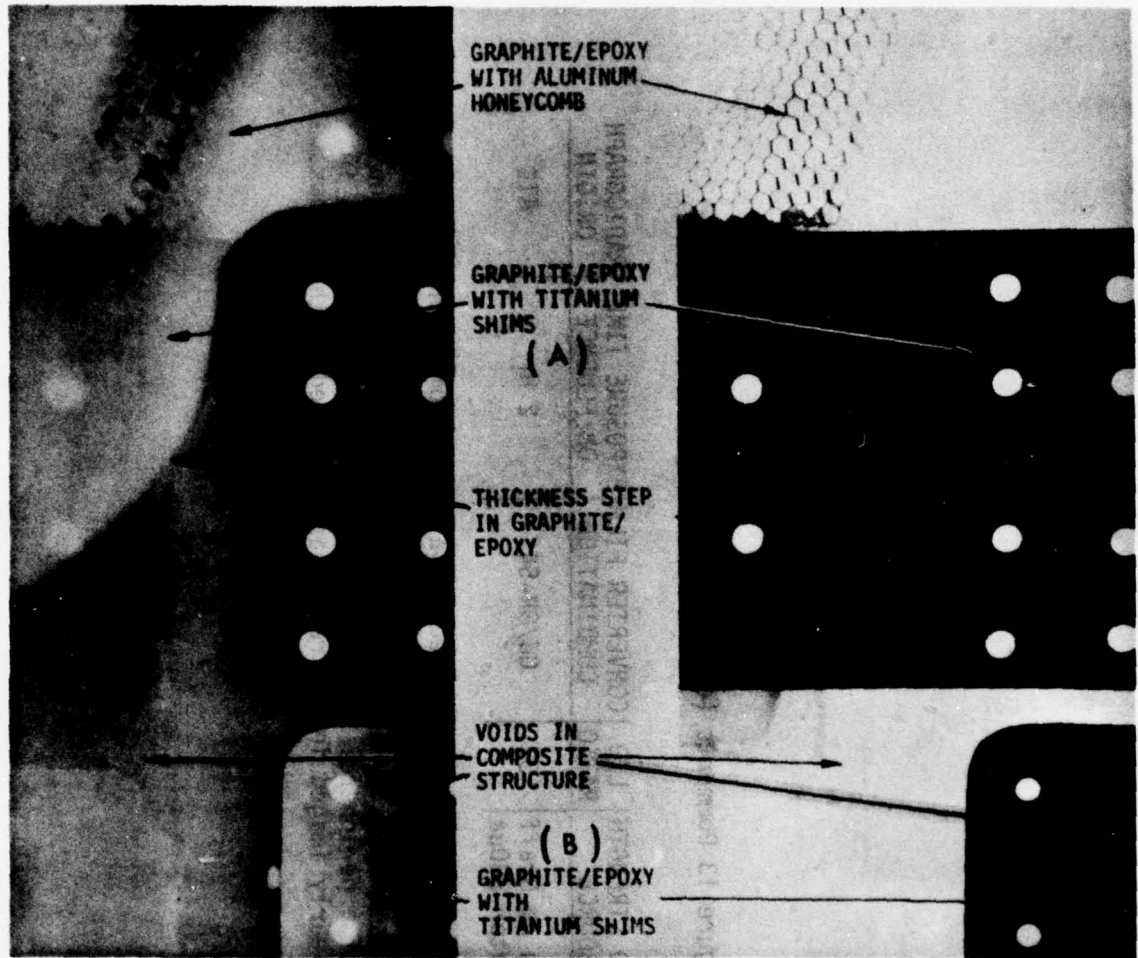


Figure 11 - Fast Film/Converter Neutron Radiograph of Thick Laminated Skin-to-Spar Joint in Aircraft Wing Section



NEUTRON

X-RAY

SPECIMEN THICKNESS	TYPE AND STRENGTH OF SOURCE	L/D RATIO	CONVERTER FILM COMBINATION	EXPOSURE TIME OR FLUENCE	RADIOGRAPH ORIGIN
.75"	²⁵² Cf, 3.2 mg	16	Gd/SR-54	59 Hr	ATC

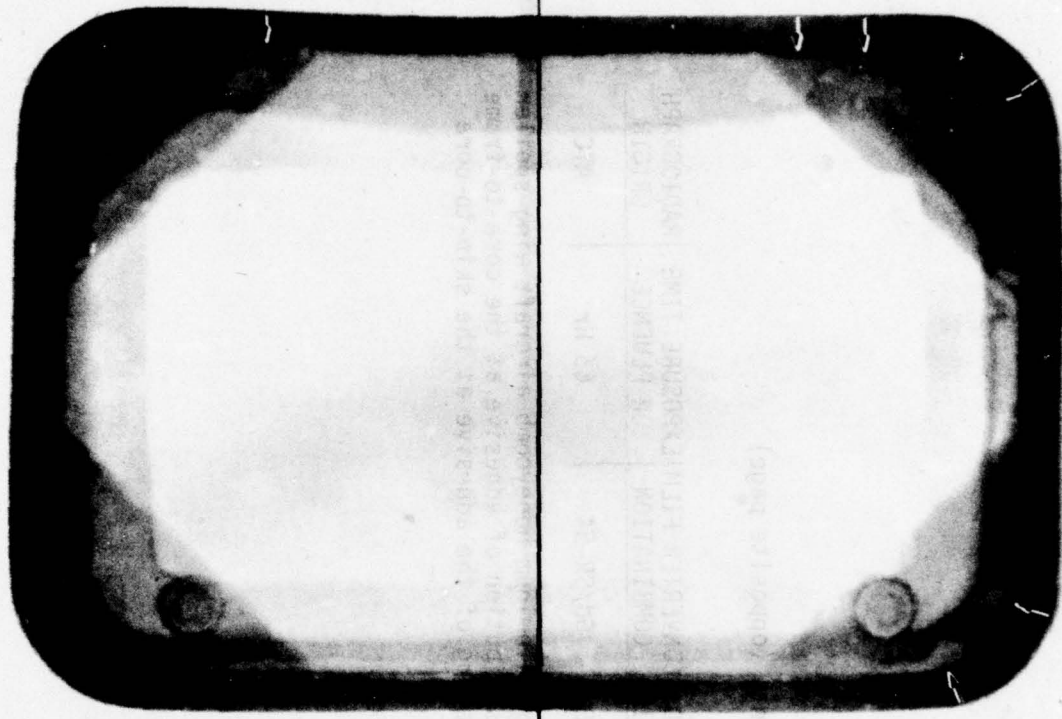
The specimen was an adhesively bonded hybrid composite/metal wing skin structure which incorporated graphite-epoxy composite material, aluminum honeycomb, and titanium shims. The noteworthy feature here is that neutron radiography enables one to image the adhesive bond line which bonds the titanium shims into the structure. Voids in this bond line are seen at A and B. The X-ray radiograph at the right shows the boundaries of the titanium shims, since the titanium was essentially opaque to the X-ray beam used for this exposure.

Figure 12 - Neutron Radiograph of Hybrid Metal/Composite Wing Skin Structure

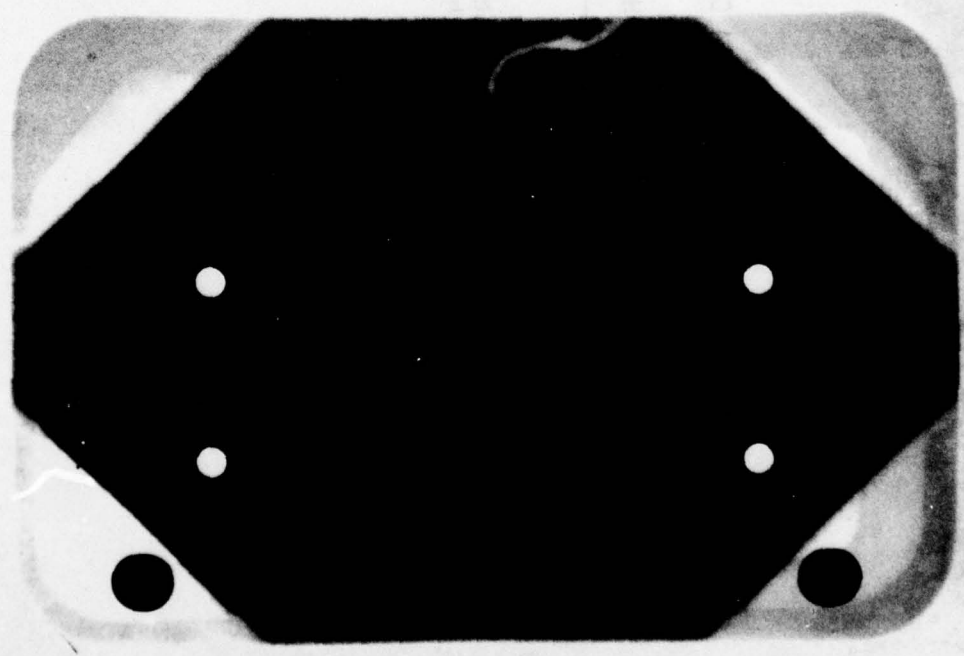
Figure 13 Comments (opposite page)

SPECIMEN THICKNESS	TYPE AND STRENGTH OF SOURCE	L/D RATIO	CONVERTER FILM COMBINATION	EXPOSURE TIME OR FLUENCE	RADIOGRAPH ORIGIN
.625"	3Mev Van de Graff accelerator 280µa	37	Gd/SR-54	2 Hr	ATC

This radiograph shows the results of inspecting a ramjet combustor port cover assembly. This component is comprised of a curved aluminum plate with a phenolic fiberglass frame assembly adhesively bonded at the edge of and on both sides near the edge of a peripheral flange in the plate. Adhesive flaws in this bond line are clearly imaged in the radiograph as noted by the arrows.



**NEUTRON RADIOGRAPHIC
INSPECTION FOR BOND FLAWS**



**CONVENTIONAL RADIOGRAPHIC
INSPECTION - X-RAY**

Figure 13 - Neutron Radiograph of Missile Combustor Port Cover Assembly

ИЗДЕЛИЮ - X-87A
 КОМПЛЕКТОВЫЙ РАДИОГРАФИЧЕСКИЙ
 ИЗДЕЛИЮ - X-87A
 КОМПЛЕКТОВЫЙ РАДИОГРАФИЧЕСКИЙ

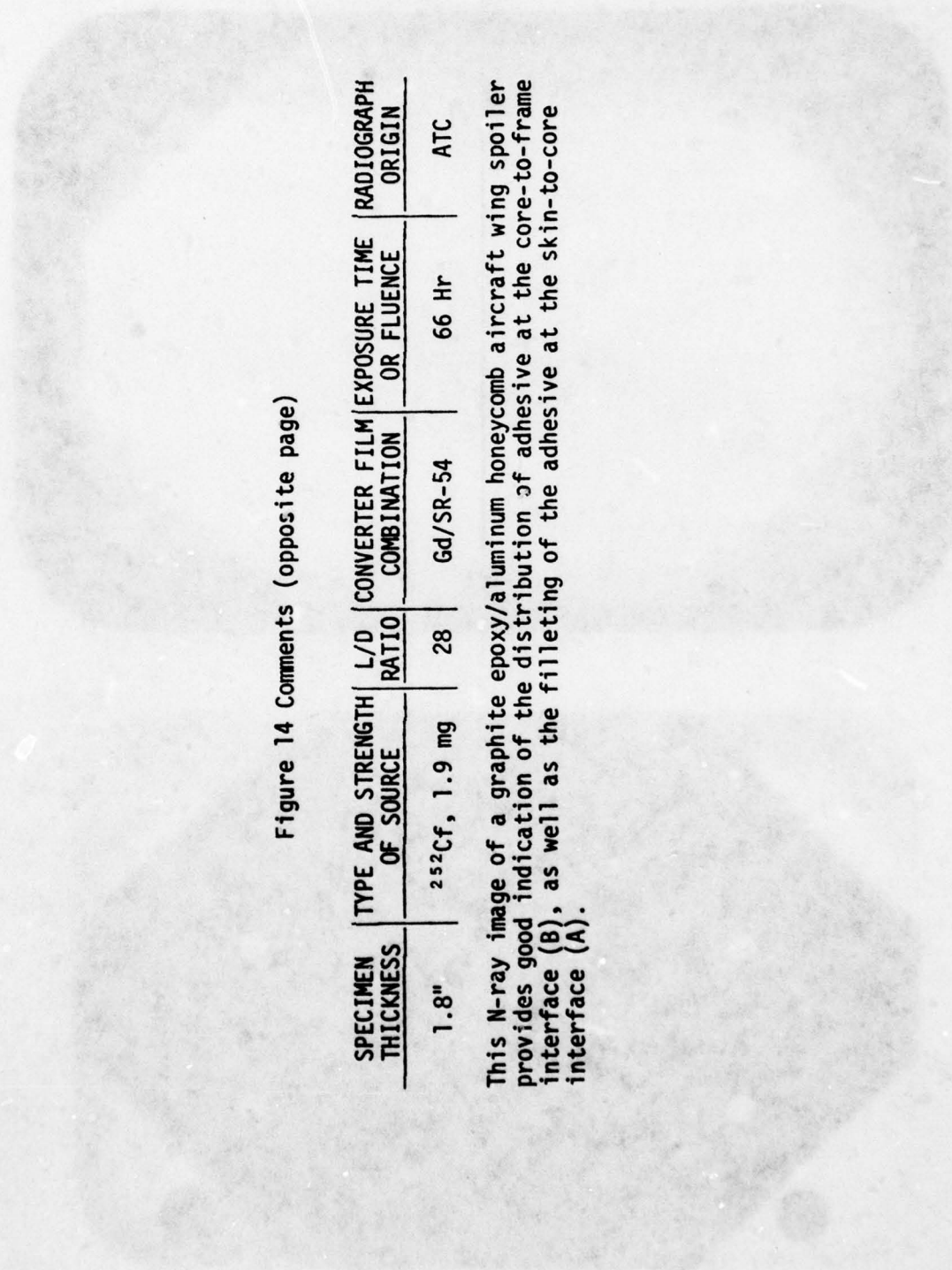


Figure 14 Comments (opposite page)

SPECIMEN THICKNESS	TYPE AND STRENGTH OF SOURCE	L/D RATIO	CONVERTER FILM COMBINATION	EXPOSURE TIME OR FLUENCE	RADIOGRAPH ORIGIN
1.8"	^{252}Cf , 1.9 mg	28	Gd/SR-54	66 Hr	ATC

This N-ray image of a graphite epoxy/aluminum honeycomb aircraft wing spoiler provides good indication of the distribution of adhesive at the core-to-frame interface (B), as well as the filleting of the adhesive at the skin-to-core interface (A).

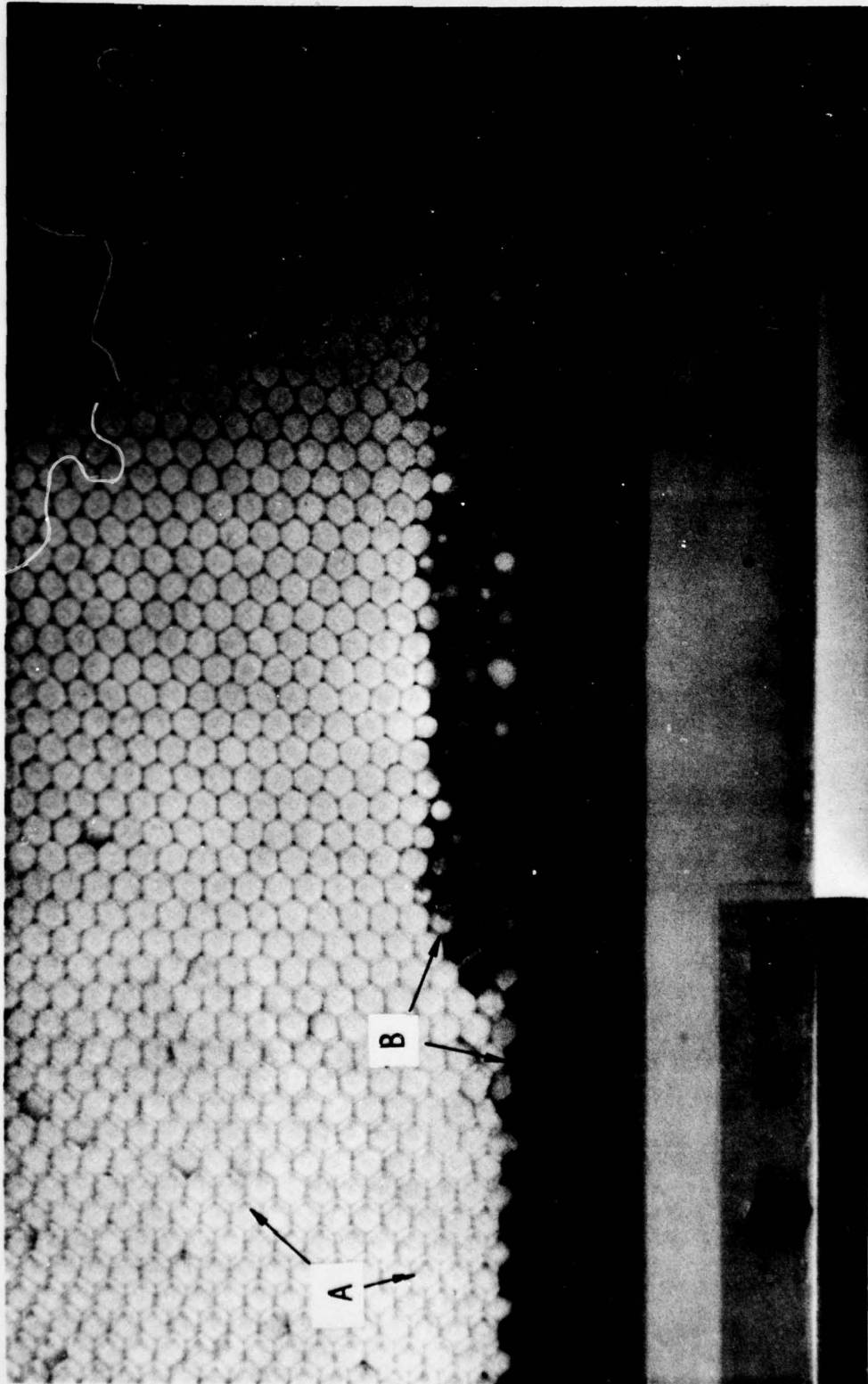
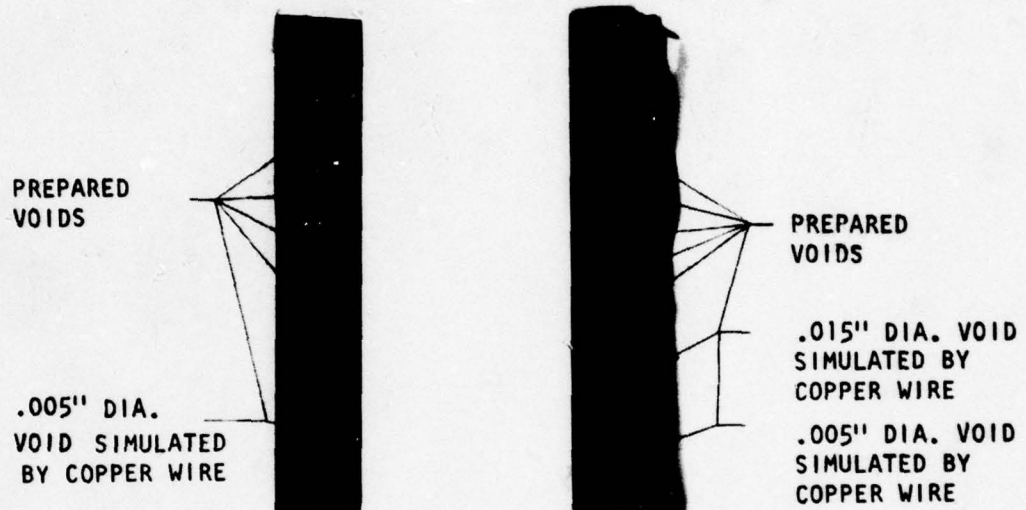


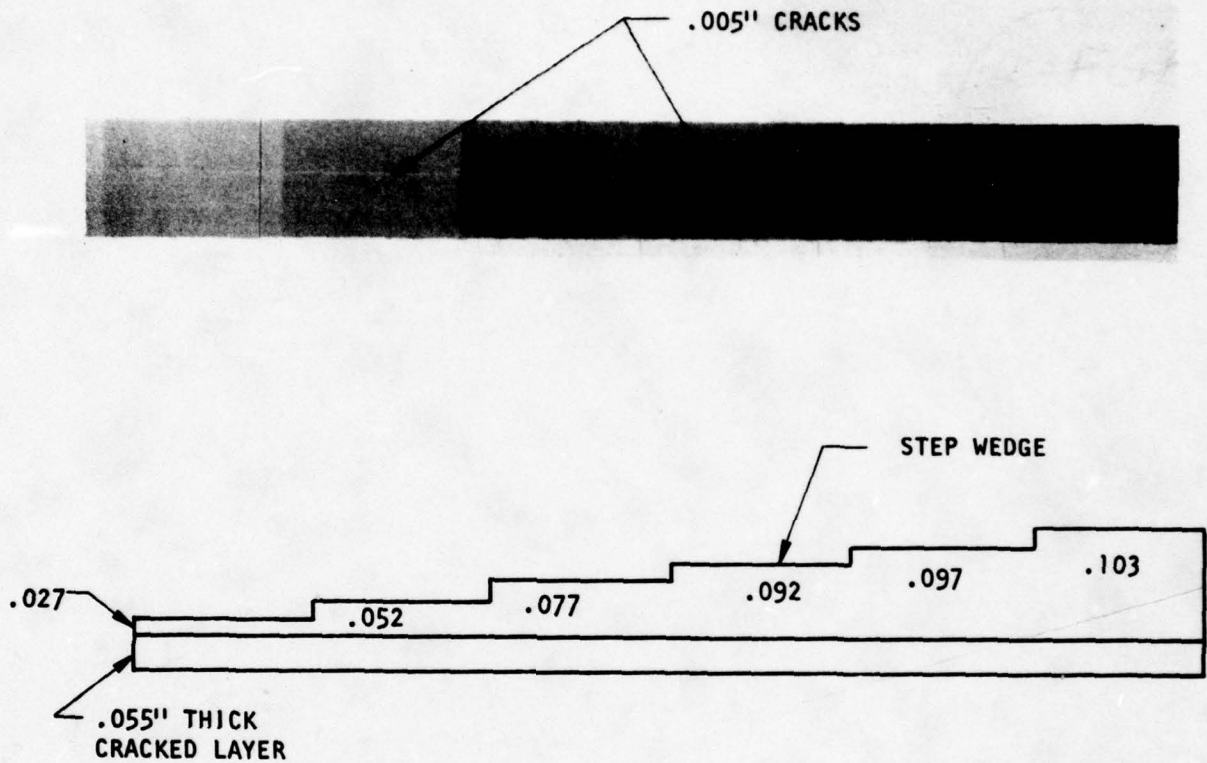
Figure 14 - Neutron Radiograph of Composite Skin/Aluminum Honeycomb Aircraft Wing Spoiler



SPECIMEN THICKNESS	TYPE AND STRENGTH OF SOURCE	L/D RATIO	CONVERTER FILM COMBINATION	EXPOSURE TIME OR FLUENCE	RADIOGRAPH ORIGIN
A-.2" Gr/Ep B-.2" Gr/Ep+ .065"Ti	²⁵² Cf, 2.5 mg	16	Gd/SR-54	16 Hr	ATC

Voids in thin bond lines joining composite members can be radiographically imaged by use of a neutron opaque additive in the adhesive. This radiograph is illustrative of the contrast and resolution available when this technique is used. Void sizes, which are approximately full-scale, are as indicated on the print for simulated voids built into the specimen. The specimen at the left contained no metallic inserts while the one to the right contained a .065-inch titanium shim. These specimens were prepared from 0.10-inch graphite/epoxy panels joined by .005-inch bond lines.

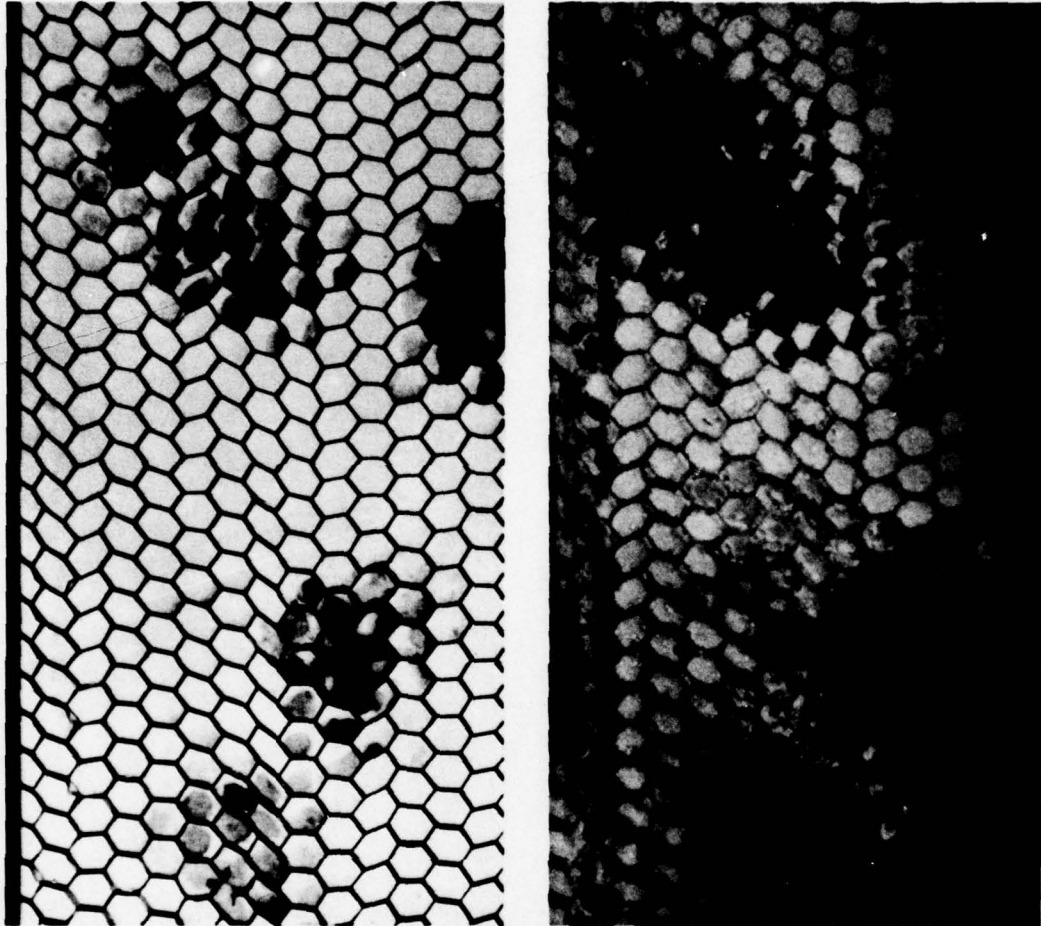
Figure 15 - Neutron Radiograph of Bonded Composite (Graphite Epoxy) Specimens



SPECIMEN THICKNESS	TYPE AND STRENGTH OF SOURCE	L/D RATIO	CONVERTER FILM COMBINATION	EXPOSURE TIME OR FLUENCE	RADIOGRAPH ORIGIN
Step .082" to .158"	²⁵² Cf, 2.5 mg	16	Gd/SR-54	18 Hr	ATC

This neutron radiograph images .005-inch cracks in a .055-inch thick graphite epoxy sheet masked by a graphite epoxy step wedge having thicknesses ranging from .027 to .103 inch. This specimen simulated hidden internal crack damage.

Figure 16 - Neutron Radiograph of Graphite Epoxy Specimen Containing Cracks in Sublayer



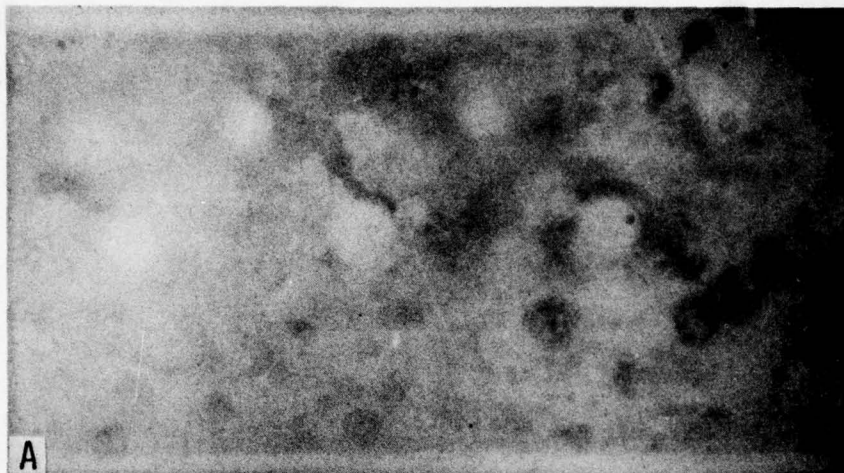
X-RAY

NEUTRON

SPECIMEN THICKNESS	TYPE AND STRENGTH OF SOURCE	L/D RATIO	CONVERTER FILM COMBINATION	EXPOSURE TIME OR FLUENCE	RADIOGRAPH ORIGIN
-	^{252}Cf , 0.7 mg	18	Gd/SR-54	71 Hr	ATC

Corrosion damage in aluminum honeycomb at the skin interface is often detectable as a total absence of adhesive filleting, as shown in this radiograph of an aileron section on which extensive repairs had been made. When significant quantities of corrosion products are present, they are shadow imaged directly by neutron attenuation.

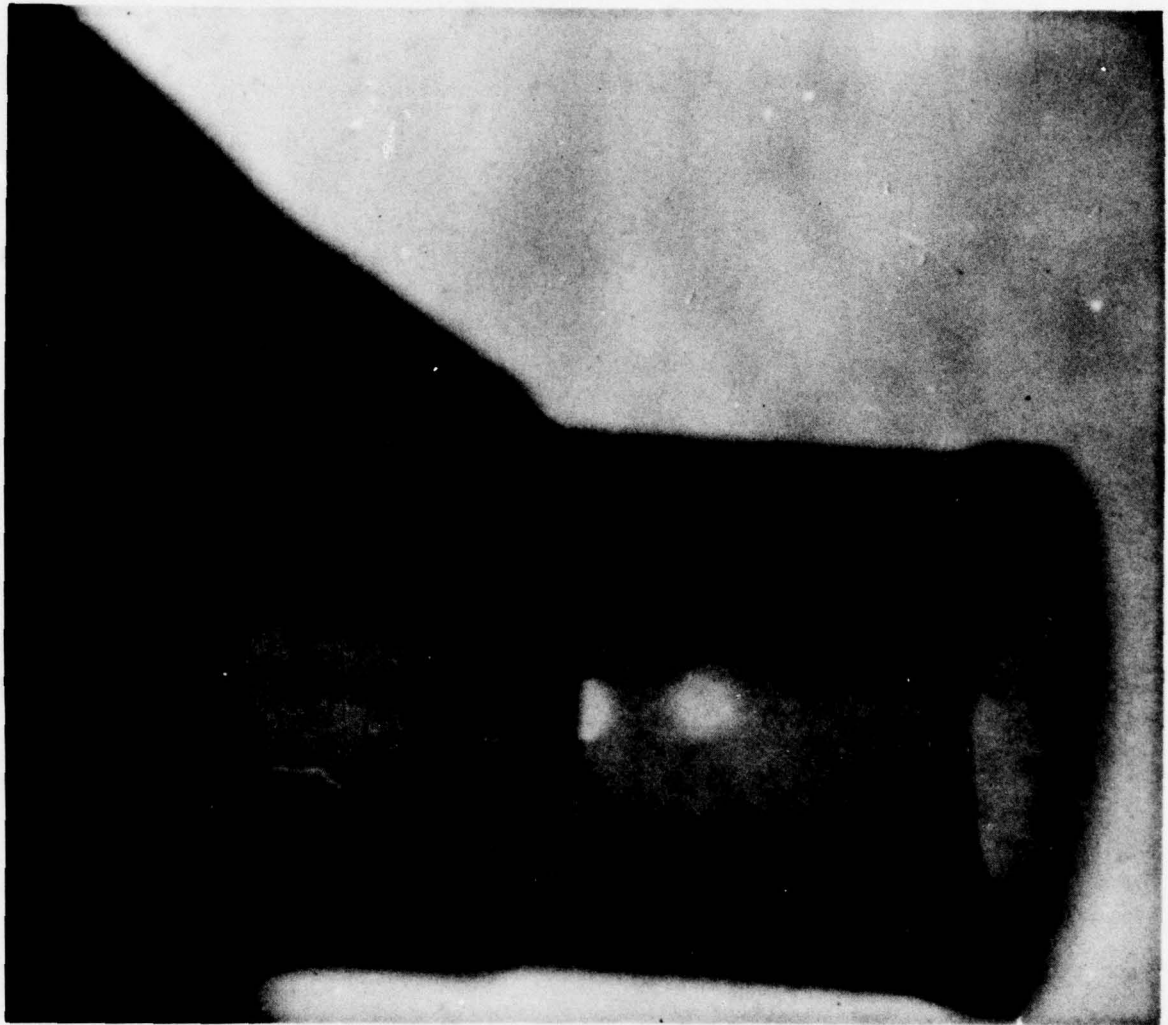
Figure 17 - Neutron Radiograph of Corrosion-Damaged Aileron Section



SPECIMEN THICKNESS	TYPE AND STRENGTH OF SOURCE	L/D RATIO	CONVERTER FILM COMBINATION	EXPOSURE TIME OR FLUENCE	RADIOGRAPH ORIGIN
.023" + .037"	²⁵² Cf, 1.5 mg	16 25	Gd/SR-54	31 Hr 65 Hr	ATC ATC

Shown here is a comparison of neutron radiographs of a small section of a highly corroded F-8 aircraft fuselage panel: (A) in "as-was" condition, (B) after removal of all surface corrosion from a portion of the specimen. The portion to the right of the arrow in (B) corresponds to that portion which is free of surface corrosion and images the exfoliation (dark areas) surrounding the rivet holes and spot-welds.

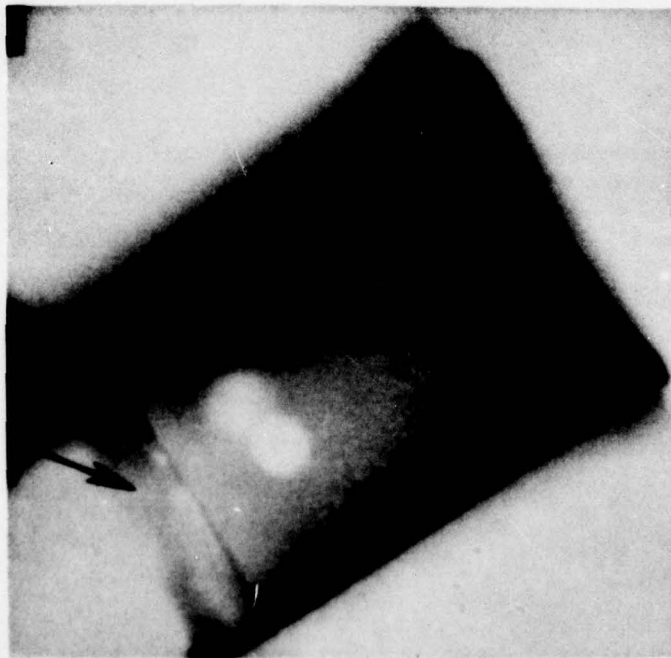
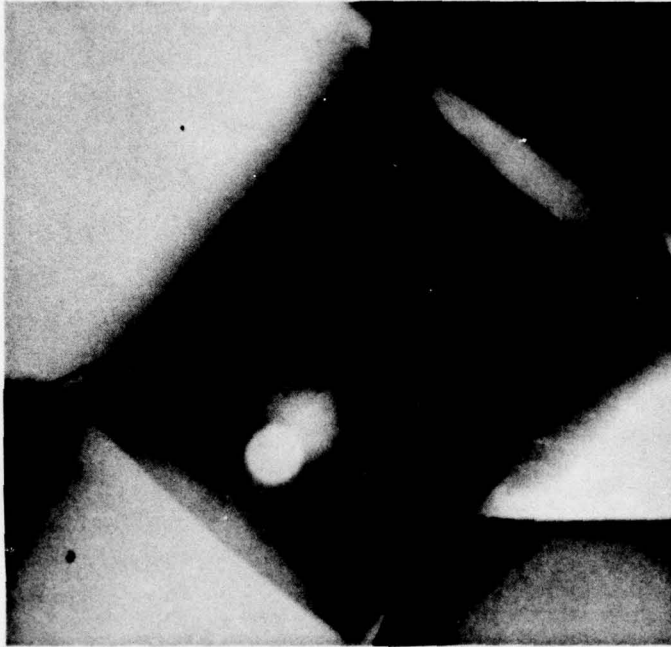
Figure 18 - Neutron Radiograph of Corroded F-8 Fuselage Panel



SPECIMEN THICKNESS	TYPE AND STRENGTH OF SOURCE	L/D RATIO	CONVERTER FILM COMBINATION	EXPOSURE TIME OR FLUENCE	RADIOGRAPH ORIGIN
Shell .038" Aluminum + Bushing	²⁵² Cf	17	Gd/AA	1.3 x 10 ⁸ n/cm ²	IRT

This radiograph is the result of N-ray inspection of the nose landing gear housing from an A-7 aircraft. Of primary concern was the inspection for corrosion on the inner wall of the aluminum housing which is hidden by the bronze bushings. The result shown here images corrosion products on that inner surface which houses the bushing.

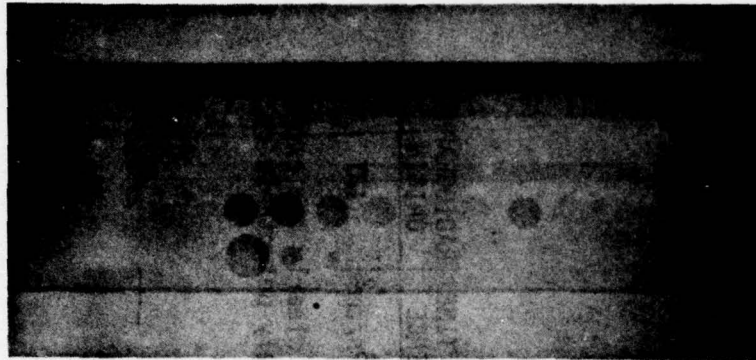
Figure 19 - Neutron Radiograph of A-7 Nose-Gear Housing



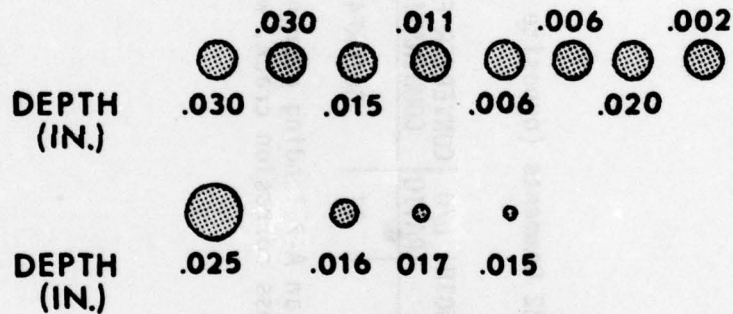
SPECIMEN THICKNESS	TYPE AND STRENGTH OF SOURCE	L/D RATIO	CONVERTER FILM COMBINATION	EXPOSURE TIME OR FLUENCE	RADIOGRAPH ORIGIN
She11 .038" Aluminum + Bushing	²⁵² Cf, 3.2 mg	16	Gd/SR	16 Hr	ATC

This radiograph resulted from inspection of another A-7 nose-gear housing before removal of the trunnion bushing. The dark spots are interpreted as clusters of sealant material or cadmium plating distributed in this manner during insertion of the bushing into the assembly.

Figure 20 - Neutron Radiograph of Trunnion Bushing Area in A-7 Nose-Gear Housing



CORROSION SIMULATED BY $Al(OH)_3$



HOLE PATTERN

SPECIMEN THICKNESS	TYPE AND STRENGTH OF SOURCE	L/D RATIO	CONVERTER FILM COMBINATION	EXPOSURE TIME OR FLUENCE	RADIOGRAPH ORIGIN
Shell .038" Aluminum + Bushing	Van de Graaff accelerator, 280µa	18	Gd/M	20 Min	ATC

An indication of resolution and sensitivity for detection of corrosion in the A-7 nose gear at the housing/bushing interface is shown in this radiograph. A corrosion standard for inspecting the upper 5-inch main bushing interface, prepared by drilling holes of various diameters and depths in the inner housing wall and filling with $Al(OH)_3$ to simulate corrosion, was radiographed with bushing in place to yield this result. Depths and diameters of the filled holes are as indicated by the numbers.

Figure 21 - Neutron Radiograph of A-7 Nose-Gear Corrosion Reference Specimen for Main Bushing Outer Housing

Figure 22 Comments (opposite page)

SPECIMEN THICKNESS	TYPE AND STRENGTH OF SOURCE	L/D RATIO	CONVERTER FILM COMBINATION	EXPOSURE TIME OR FLUENCE	RADIOGRAPH ORIGIN
-	²⁵² Cf	17	Gd/GAF400	4.4 x 10 ⁸ n/cm ²	IRT

This neutron radiograph of an A-7 landing gear housing shows clearly the extent, shape, and nature of a stress corrosion crack, which was barely detectable by visual inspection.

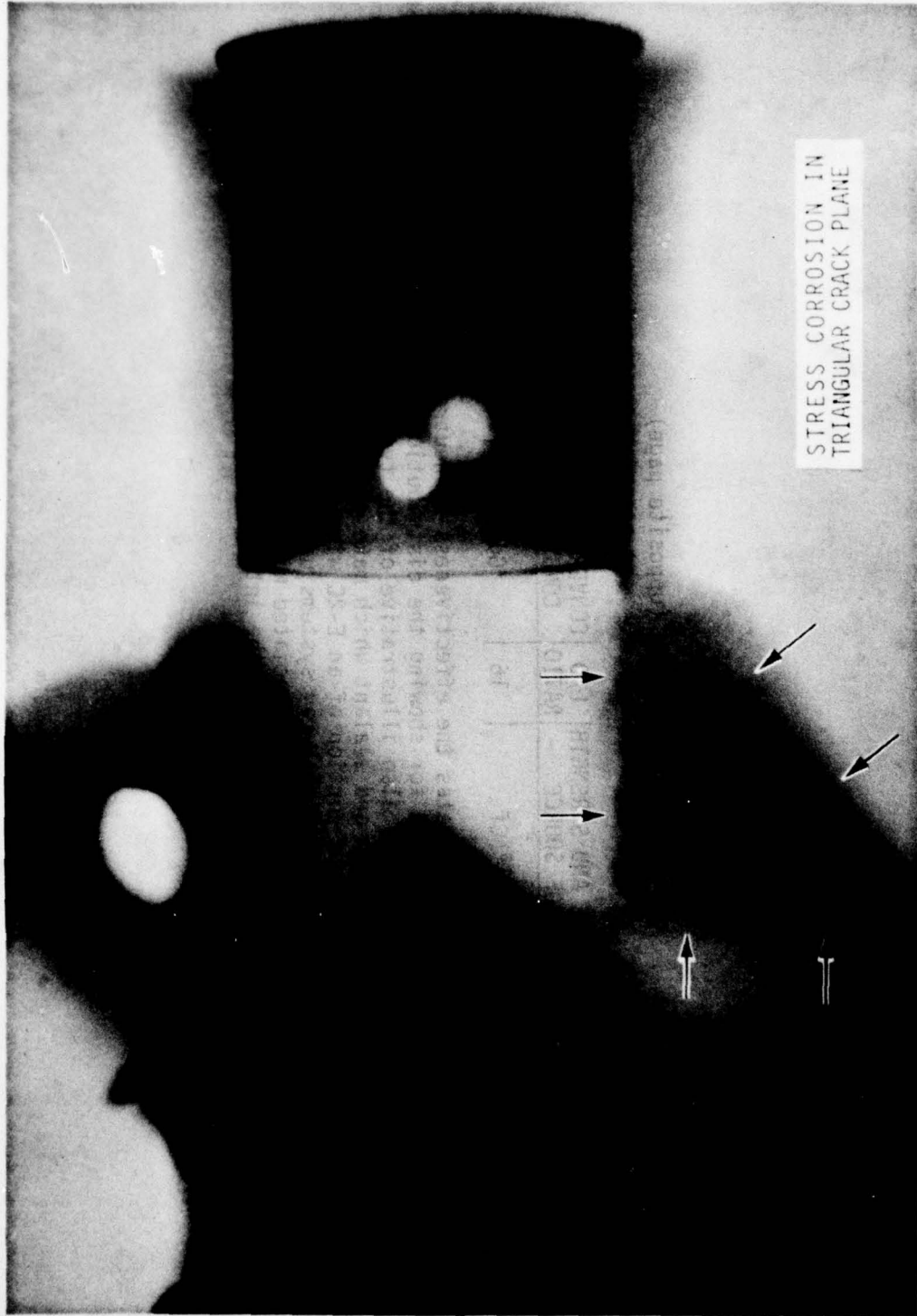


Figure 22 - Neutron Radiograph of Stress Corrosion Crack in A-7
Nose-gear Housing

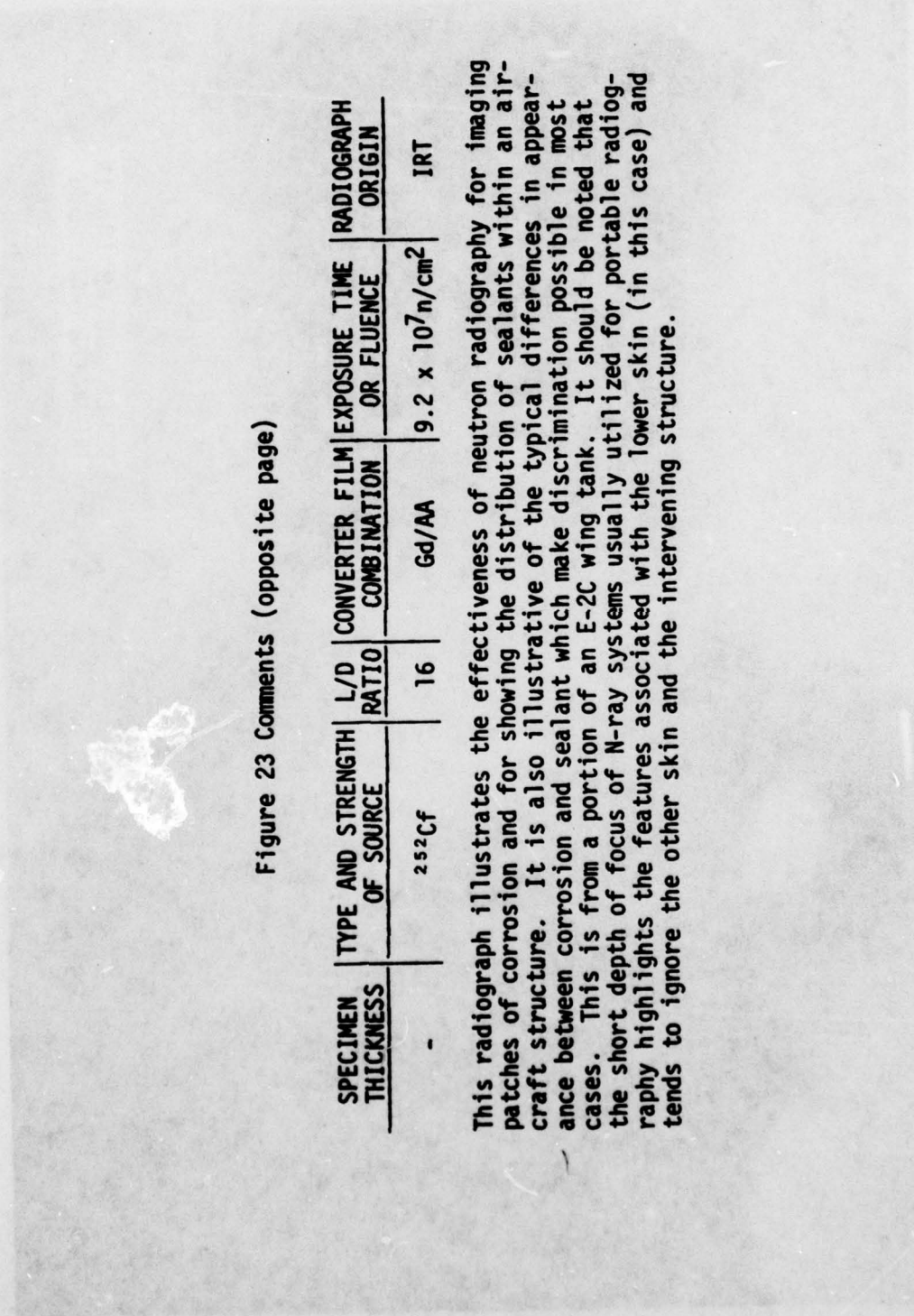


Figure 23 Comments (opposite page)

SPECIMEN THICKNESS	TYPE AND STRENGTH OF SOURCE	L/D RATIO	CONVERTER FILM COMBINATION	EXPOSURE TIME OR FLUENCE	RADIOGRAPH ORIGIN
-	^{252}Cf	16	Gd/AA	$9.2 \times 10^7 \text{ n/cm}^2$	IRT

This radiograph illustrates the effectiveness of neutron radiography for imaging patches of corrosion and for showing the distribution of sealants within an aircraft structure. It is also illustrative of the typical differences in appearance between corrosion and sealant which make discrimination possible in most cases. This is from a portion of an E-2C wing tank. It should be noted that the short depth of focus of N-ray systems usually utilized for portable radiography highlights the features associated with the lower skin (in this case) and tends to ignore the other skin and the intervening structure.

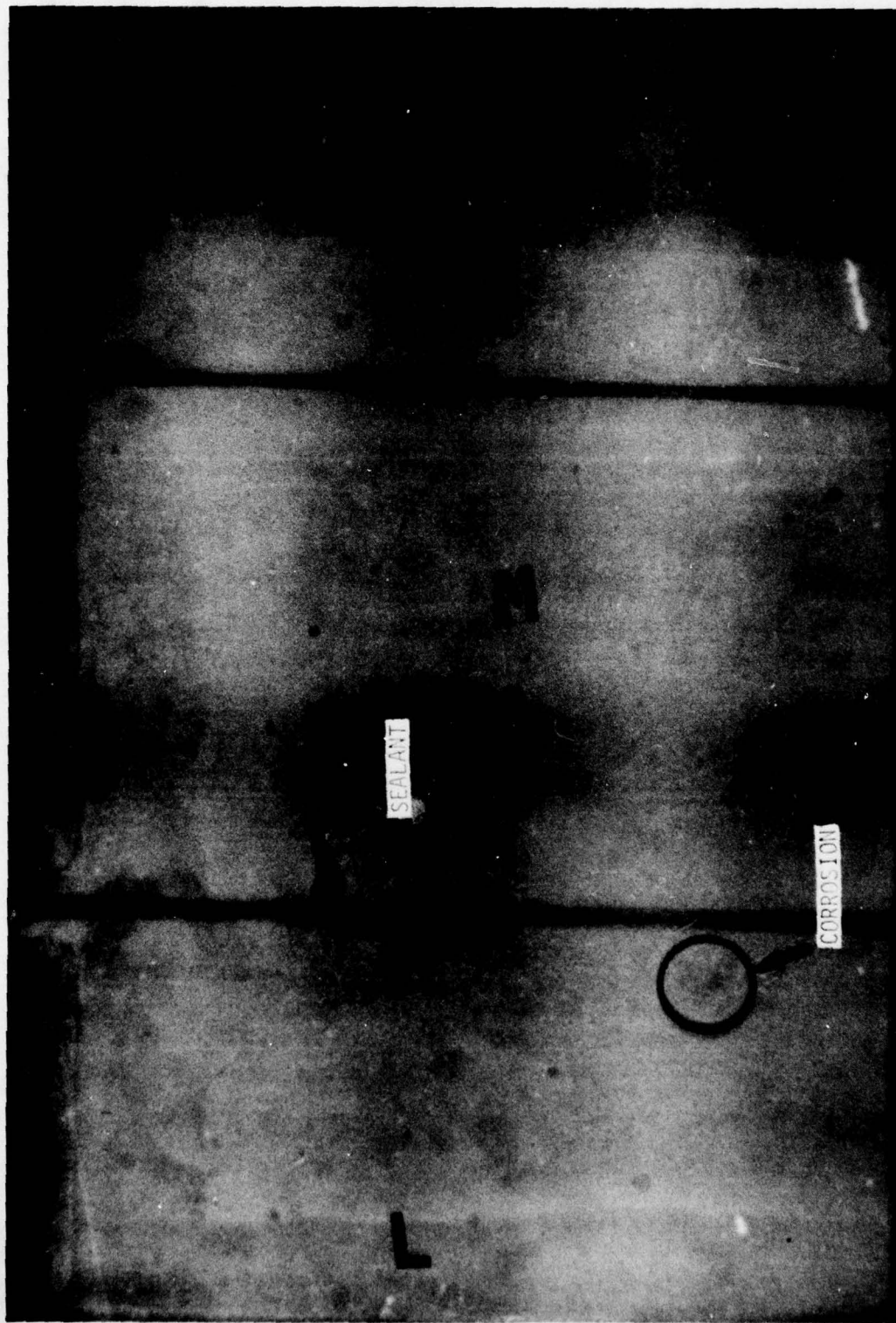
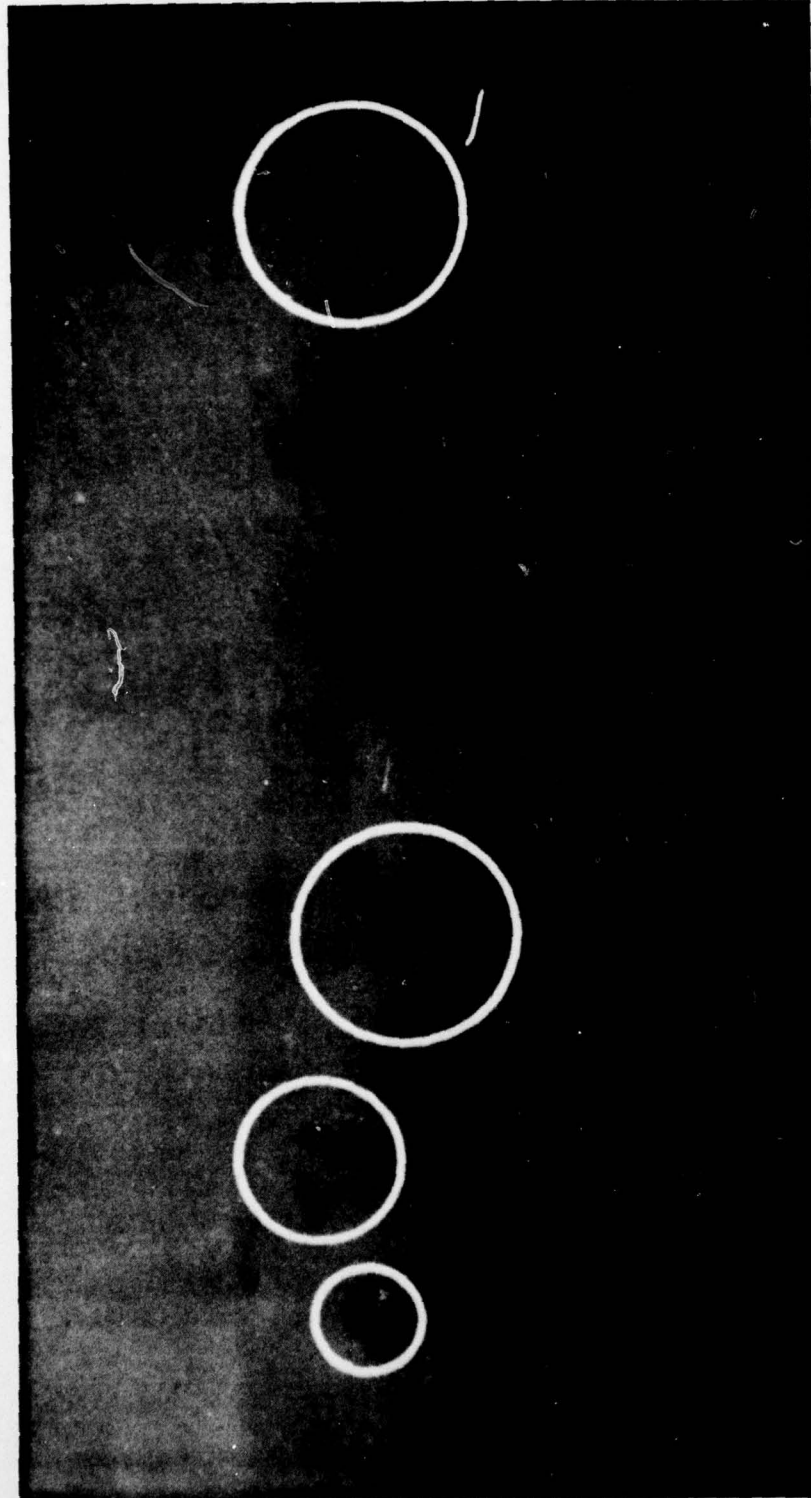


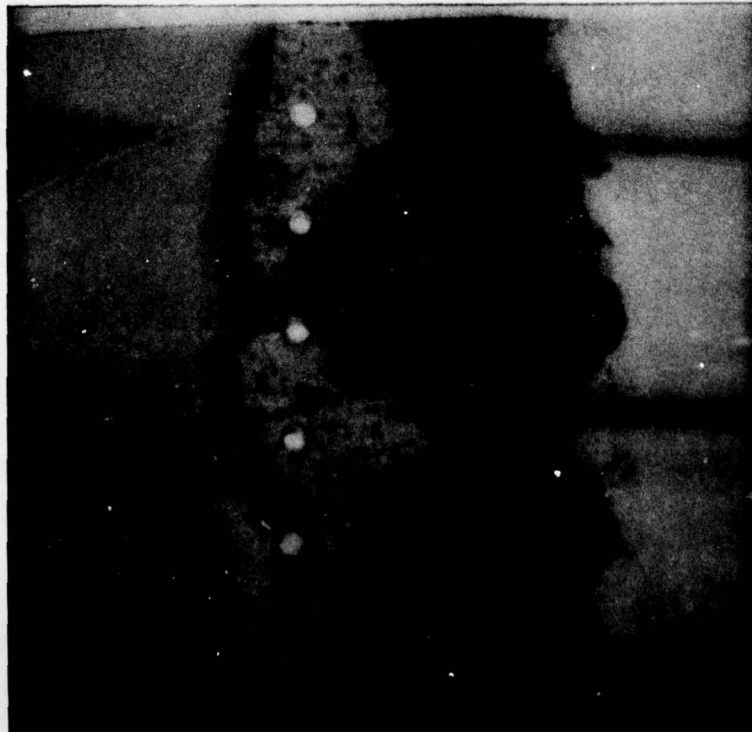
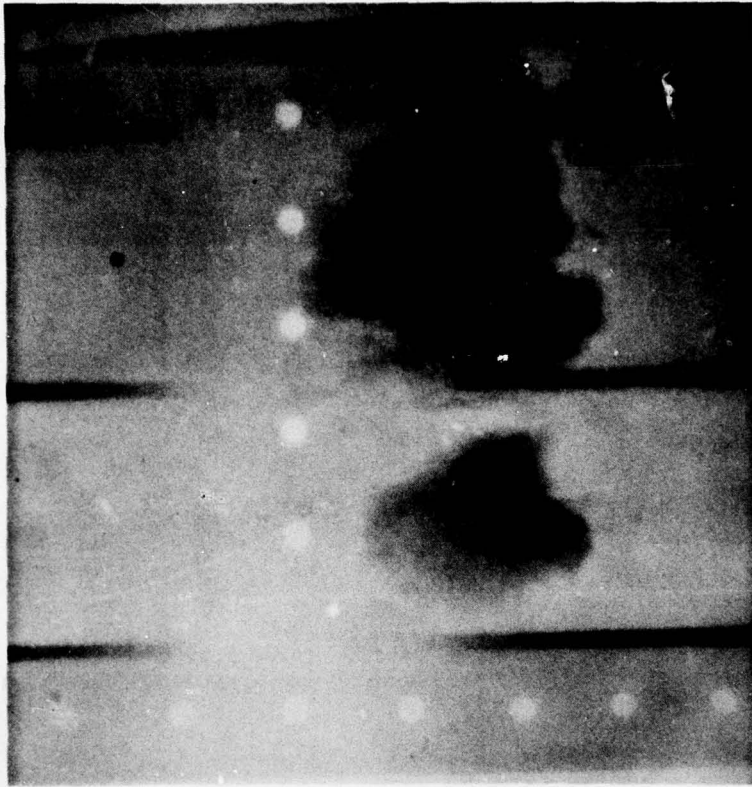
Figure 23 - Neutron Radiograph of E-2C Wing-Tank Structure



SPECIMEN THICKNESS	TYPE AND STRENGTH OF SOURCE	L/D RATIO	CONVERTER FILM COMBINATION	EXPOSURE TIME OR FLUENCE	RADIOGRAPH ORIGIN
-	²⁵² Cf	16	Gd/AA	9.3 x 10 ⁷ n/cm ²	IRT

This radiograph is an example of neutron imaging of corrosion in the presence of sealant materials, where the corrosion is imaged through the sealant.

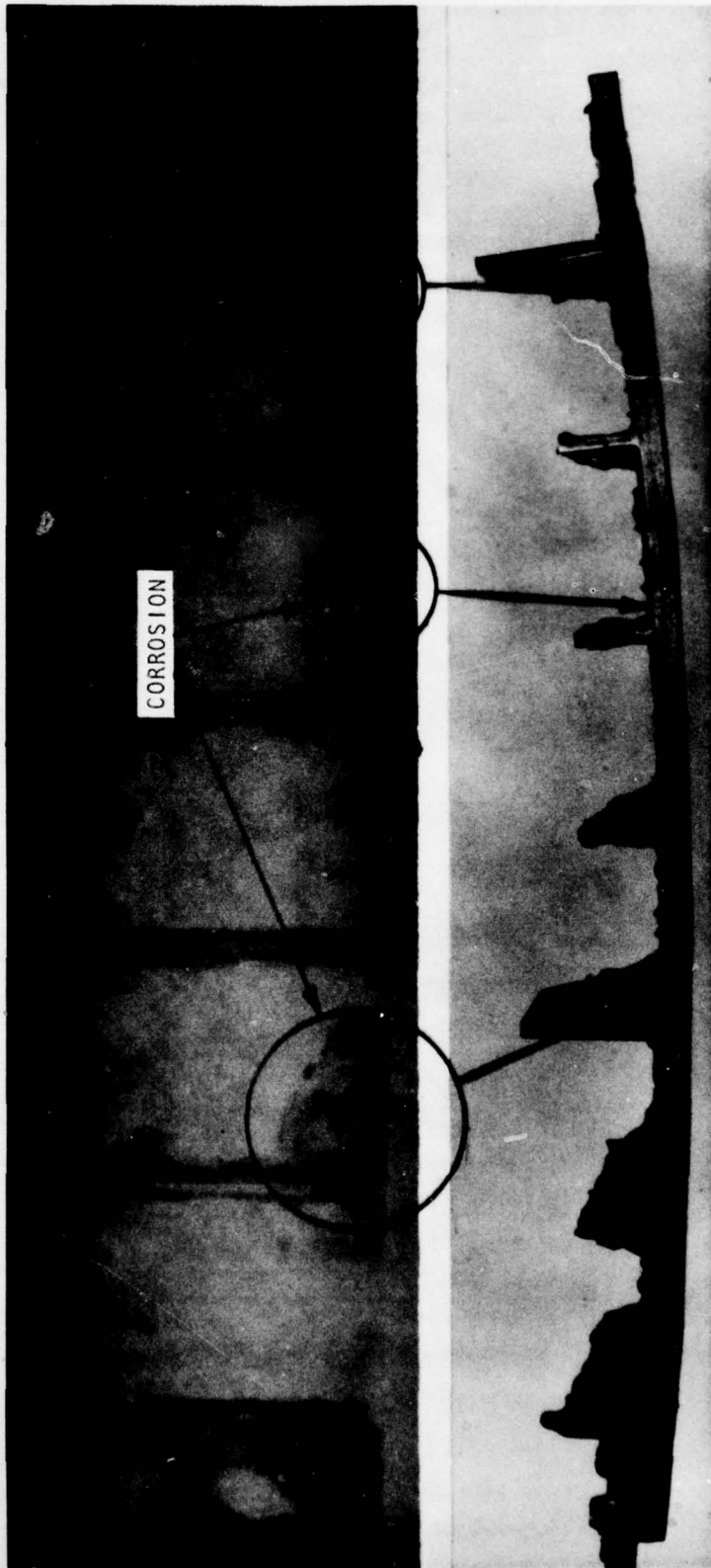
Figure 24 - Neutron Radiograph of E-2C Aircraft Wing Fuel Tank Structure



SPECIMEN THICKNESS	TYPE AND STRENGTH OF SOURCE	L/D RATIO	CONVERTER FILM COMBINATION	EXPOSURE TIME OR FLUENCE	RADIOGRAPH ORIGIN
-	²⁵² Cf	22	Gd/M	5.0 x 10 ⁸ n/cm ²	IRT

The radiograph on the right was obtained in the usual manner, and the one on the left with the use of a penetrant. The intergranular corrosion is seen to extend beyond the rivet holes, clearly explaining the cause of a fuel leak previously found in the structure.

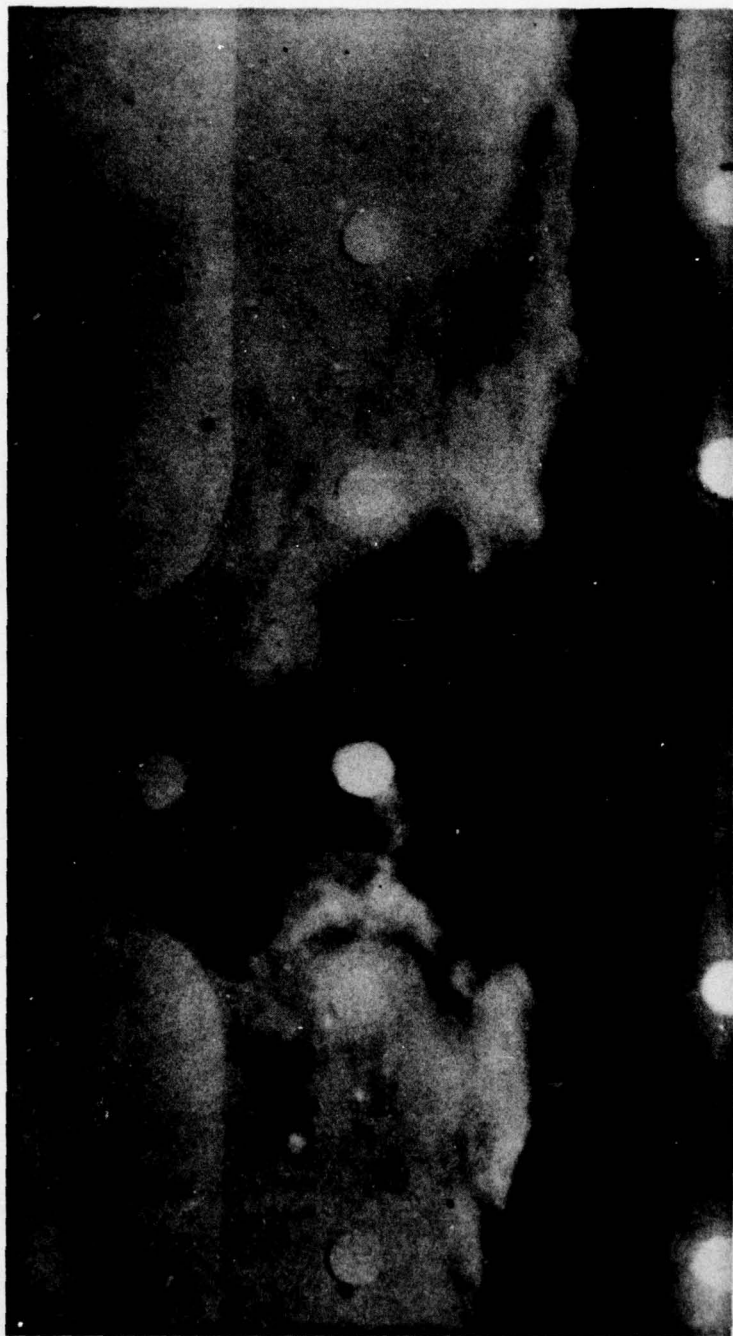
Figure 25 - Neutron Radiograph of C-130 Wing Structure



SPECIMEN THICKNESS	TYPE AND STRENGTH OF SOURCE	L/D RATIO	CONVERTER FILM COMBINATION	EXPOSURE TIME OR FLUENCE	RADIOGRAPH ORIGIN
-	^{252}Cf	22	Gd/M	$5.0 \times 10^9 \text{ n/cm}^2$	IRT

Intergranular corrosion in the lower skin of a C-130 aircraft wing is imaged. Visual confirmation of this result was achieved upon sectioning of the skin, as seen in the edge photograph on the top.

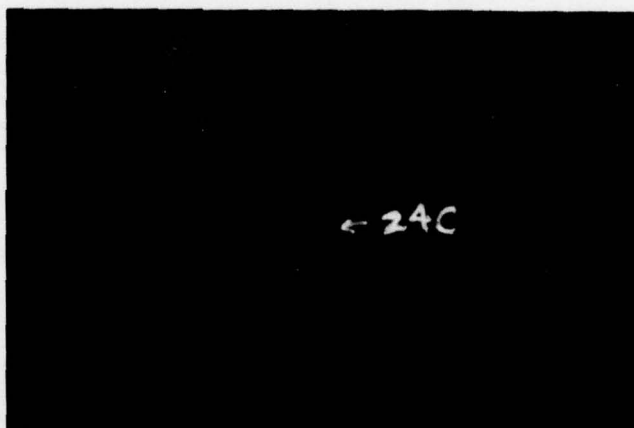
Figure 26 - Neutron Radiograph of Lower Skin of C-130 Aircraft Wing



SPECIMEN THICKNESS	TYPE AND STRENGTH OF SOURCE	L/D RATIO	CONVERTER FILM COMBINATION	EXPOSURE TIME OR FLUENCE	RADIOGRAF. ORIGIN
-	²⁵² Cf	24	Gd/SR	2.4 x 10 ⁹ n/cm ²	IRT

This neutron radiograph (enlarged) of a section of an F-4 torque box panel illustrates the high contrast attainable in some instances in detecting severe corrosion attack (dark area between the two rows of fastener holes and around one of the upper holes).

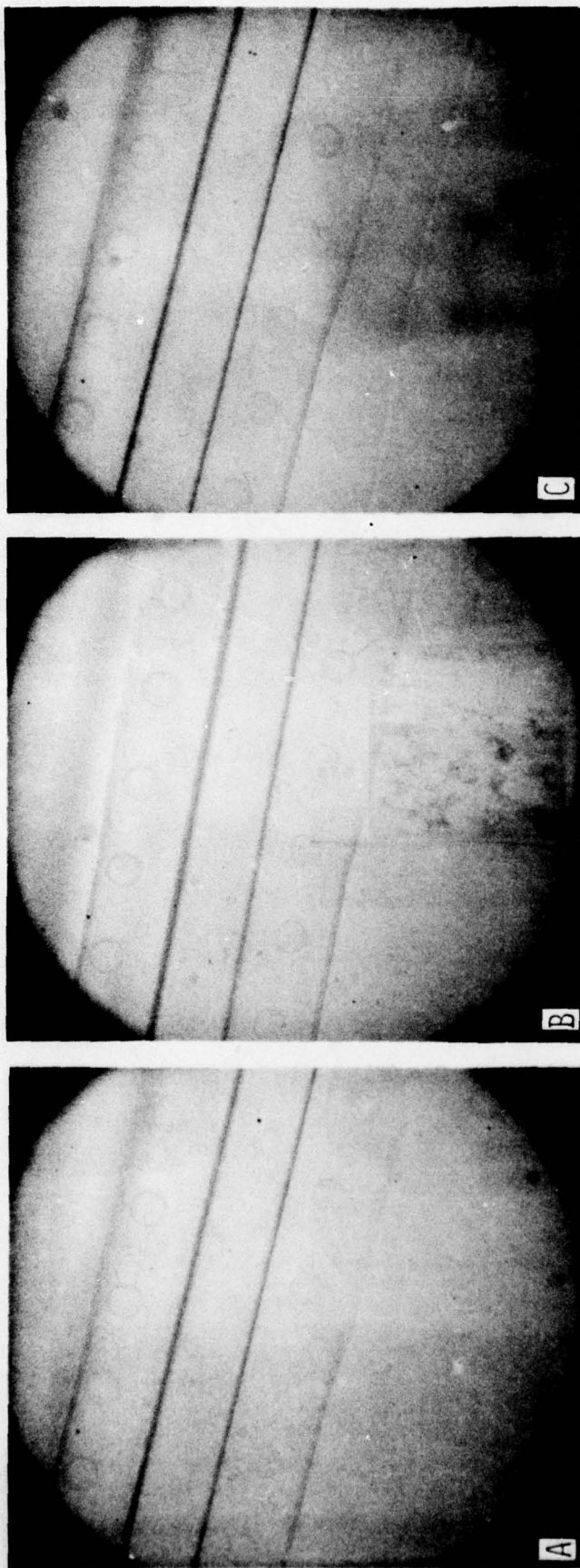
Figure 27 - Neutron Radiograph of F-4 Torque Box Panel



SPECIMEN THICKNESS	TYPE AND STRENGTH OF SOURCE	L/D RATIO	CONVERTER FILM COMBINATION	EXPOSURE TIME OR FLUENCE	RADIOGRAPH ORIGIN
-	^{252}Cf	20	Gd/AA	$3.0 \times 10^8 \text{n/cm}^2$	IRT

A portion of A-5 aircraft skin exhibits in this neutron radiograph corrosion pits surrounded by the familiar "ragged" rings of corrosion products which are typical of corrosion attack on aluminum skins. Photographs taken before and after removal of corrosion products reveal close resemblance of radiographic image to the damage pattern in the skin (bottom view).

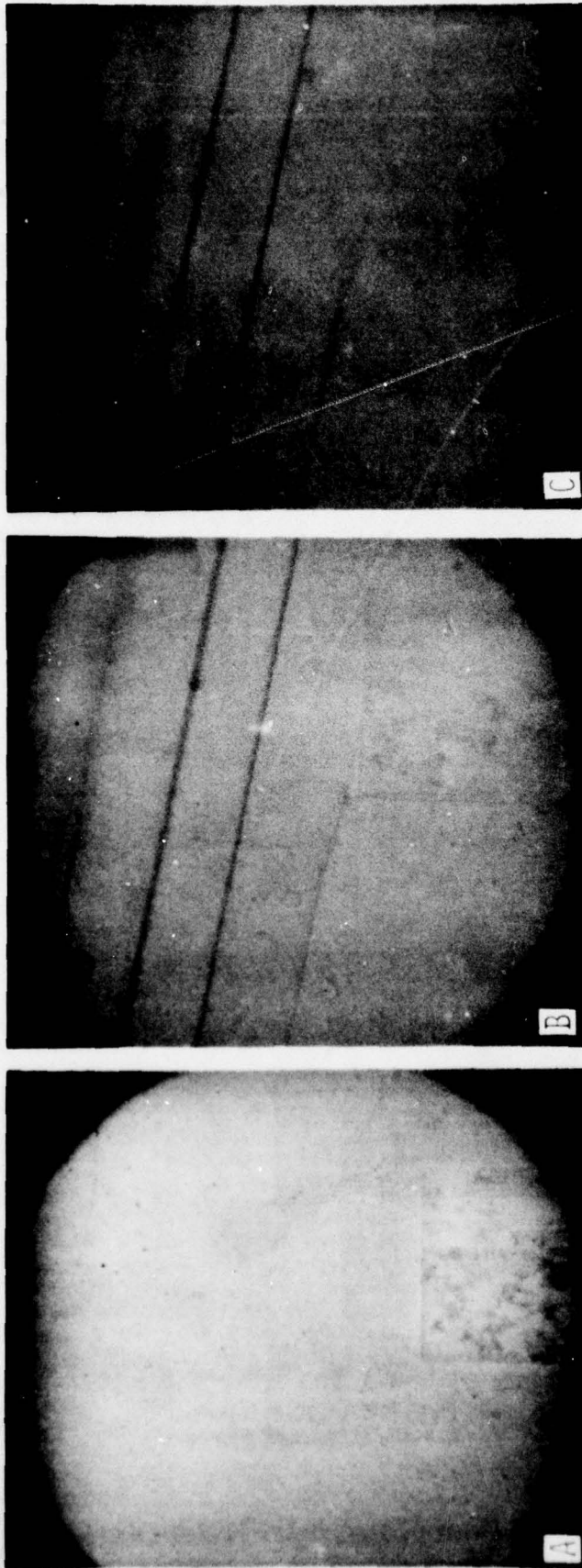
Figure 28 - Neutron Radiograph of A-5 Aircraft Skin



SPECIMEN THICKNESS	TYPE AND STRENGTH OF SOURCE	L/D RATIO	CONVERTER FILM COMBINATION	EXPOSURE TIME OR FLUENCE	RADIOGRAPH ORIGIN
Penetrimeter Steps: .125" .087" Airfoil 7.0"	10 MW Reactor	43	Gd/M	90 Sec	NBS

Radiographs of a C-2 vertical fin section (A), and of a corrosion penetrimeter attached to the fin (B,C) are shown. The penetrimeter was of aircraft-grade aluminum with nominal step thicknesses 0.125 and 0.87 inch, prepared by subjection to a supersaturated salt water spray for 6.5 hours to induce corrosion attack. Radiographs B and C were obtained with penetrimeter on the cassette side and neutron source side of the vertical fin, respectively. Due to the substantial separation (7 inches) of the penetrimeter from the film cassette in C, the corrosion pattern is unresolved in that radiograph, suggesting that for such thicknesses (greater than ~1 inch) each side should be inspected individually.

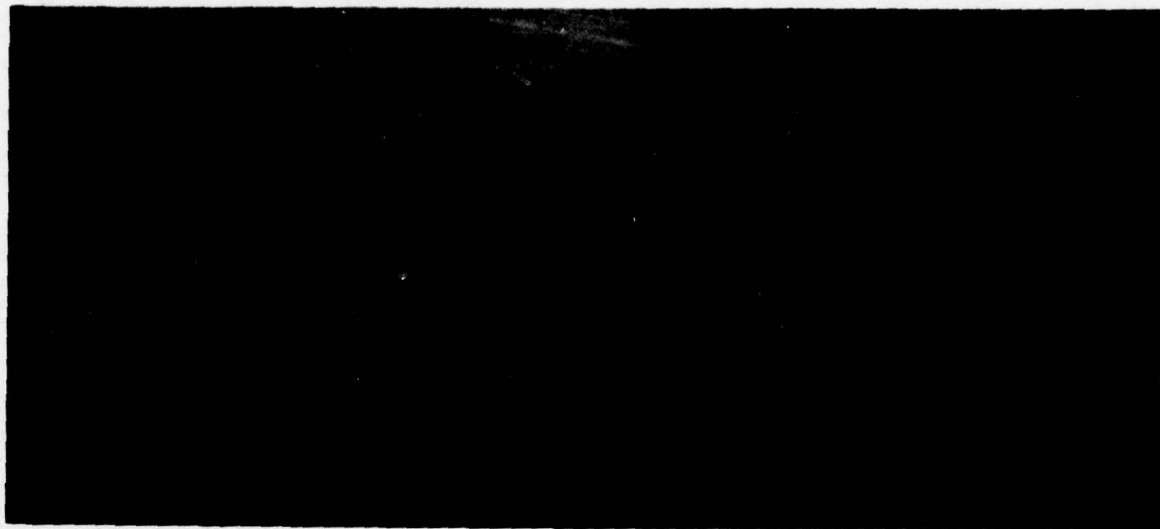
Figure 29 - Neutron Radiographs of a C-2 Vertical Fin, and Fin With Corrosion Penetrimeter Attached



SPECIMEN THICKNESS	TYPE AND STRENGTH OF SOURCE	L/D RATIO	CONVERTER FILM COMBINATION	EXPOSURE TIME OR FLUENCE	RADIOGRAPH ORIGIN
Penetrater Steps: .125" .087" Airfoil 7.0"	10 MW Reactor	43	Gd ₂ O ₂ S/M	45 Sec	NBS

The .0005-inch vapor deposited Gd converter used to radiograph the specimen of Figure 29 was replaced by a Gd₂O₂S screen to obtain these results, for comparison of converter efficiency and resolution (see Table II).

Figure 30 - Neutron Radiographs of a Corrosion Penetrater and C-2 Fin With Penetrater Attached



SPECIMEN THICKNESS	TYPE AND STRENGTH OF SOURCE	L/D RATIO	CONVERTER FILM COMBINATION	EXPOSURE TIME OR FLUENCE	RADIOGRAPH ORIGIN
-	^{252}Cf , 2 mg	20	Dy/AA	20.5 Hr	RMC

This radiograph of a corroded aircraft aluminum skin is included as an example of results using the transfer technique in which the film is exposed, not in real time by the neutron imaging beam via the converter, but by the activated converter after removal of the cassette from the specimen and neutron beam. All the preceding radiographs were obtained by the direct exposure technique.

Figure 31 - Transfer Exposure Neutron Radiograph of a Corroded Aluminum Aircraft Skin

